UNCLASSIFIED

AD NUMBER

ADB259637

NEW LIMITATION CHANGE

TO

Approved for public release, distribution unlimited

FROM

Distribution authorized to U.S. Gov't. agencies only; Proprietary Info.; Sep 99. Other requests shall be referred to U.S. Army Medical Research and Materiel Command, 504 Scott St., Fort Detrick, MD 21702-5012.

AUTHORITY

USAMRMC ltr, 8 Jan 2003

THIS PAGE IS UNCLASSIFIED

AD_____

Award Number: DAMD17-98-1-8574

TITLE: Androgen Regulation of p27 in the Normal and Neoplastic Prostate

PRINCIPAL INVESTIGATOR: Massimo Loda, M.D.

CONTRACTING ORGANIZATION: Dana Farber Cancer Institute
Boston, Massachusetts 02115

REPORT DATE: September 1999

TYPE OF REPORT: Annual

PREPARED FOR: U.S. Army Medical Research and Materiel Command
Fort Detrick, Maryland 21702-5012

DISTRIBUTION STATEMENT: Distribution authorized to U.S. Government agencies only (proprietary information, Sep 99). Other requests for this document shall be referred to U.S. Army Medical Research and Materiel Command, 504 Scott Street, Fort Detrick, Maryland 21702-5012.

The views, opinions and/or findings contained in this report are those of the author(s) and should not be construed as an official Department of the Army position, policy or decision unless so designated by other documentation.

DTIC QUALITY INSPECTED 4

20001116 025

NOTICE

USING GOVERNMENT DRAWINGS, SPECIFICATIONS, OR OTHER DATA INCLUDED IN THIS DOCUMENT FOR ANY PURPOSE OTHER THAN GOVERNMENT PROCUREMENT DOES NOT IN ANY WAY OBLIGATE THE U.S. GOVERNMENT. THE FACT THAT THE GOVERNMENT FORMULATED OR SUPPLIED THE DRAWINGS, SPECIFICATIONS, OR OTHER DATA DOES NOT LICENSE THE HOLDER OR ANY OTHER PERSON OR CORPORATION; OR CONVEY ANY RIGHTS OR PERMISSION TO MANUFACTURE, USE, OR SELL ANY PATENTED INVENTION THAT MAY RELATE TO THEM.

LIMITED RIGHTS LEGEND

Award Number: DAMD17-98-1-8574
Organization: Dana Farber Cancer Institute
Location of Limited Rights Data (Pages):

Those portions of the technical data contained in this report marked as limited rights data shall not, without the written permission of the above contractor, be (a) released or disclosed outside the government, (b) used by the Government for manufacture or, in the case of computer software documentation, for preparing the same or similar computer software, or (c) used by a party other than the Government, except that the Government may release or disclose technical data to persons outside the Government, or permit the use of technical data by such persons, if (i) such release, disclosure, or use is necessary for emergency repair or overhaul or (ii) is a release or disclosure of technical data (other than detailed manufacturing or process data) to, or use of such data by, a foreign government that is in the interest of the Government and is required for evaluational or informational purposes, provided in either case that such release, disclosure or use is made subject to a prohibition that the person to whom the data is released or disclosed may not further use, release or disclose such data, and the contractor or subcontractor or subcontractor asserting the restriction is notified of such release, disclosure or use. This legend, together with the indications of the portions of this data which are subject to such limitations, shall be included on any reproduction hereof which includes any part of the portions subject to such limitations.

THIS TECHNICAL REPORT HAS BEEN REVIEWED AND IS APPROVED FOR PUBLICATION.

Narasingha Charan Mishra
08/21/07

REPORT DOCUMENTATION PAGE

Form Approved
OMB No. 074-0188

Public reporting burden for this collection of information is estimated to average 1 hour per response, including the time for reviewing instructions, searching existing data sources, gathering and maintaining the data needed, and completing and reviewing this collection of information. Send comments regarding this burden estimate or any other aspect of this collection of information, including suggestions for reducing this burden to Washington Headquarters Services, Directorate for Information Operations and Reports, 1215 Jefferson Davis Highway, Suite 1204, Arlington, VA 22202-4302, and to the Office of Management and Budget, Paperwork Reduction Project (0704-0188), Washington, DC 20503

1. AGENCY USE ONLY (Leave blank)	2. REPORT DATE	3. REPORT TYPE AND DATES COVERED
	September 1999	Annual (1 Sep 98 - 31 Aug 99)

4. TITLE AND SUBTITLE
Androgen Regulation of p27 in the Normal and Neoplastic Prostate

5. FUNDING NUMBERS
DAMD17-98-1-8574

6. AUTHOR(S)
Massimo Loda, M.D.

7. PERFORMING ORGANIZATION NAME(S) AND ADDRESS(ES)
Dana Farber Cancer Institute
Boston, Massachusetts 02115

E-Mail: mloda@caregroup.harvard.edu

8. PERFORMING ORGANIZATION REPORT NUMBER

9. SPONSORING / MONITORING AGENCY NAME(S) AND ADDRESS(ES)
U.S. Army Medical Research and Materiel Command
Fort Detrick, Maryland 21702-5012

10. SPONSORING / MONITORING AGENCY REPORT NUMBER

11. SUPPLEMENTARY NOTES
This report contains colored photos

12a. DISTRIBUTION / AVAILABILITY STATEMENT
Distribution authorized to U.S. Government agencies only (proprietary information, Sep 99). Other requests for this document shall be referred to U.S. Army Medical Research and Materiel Command, 504 Scott Street, Fort Detrick, Maryland 21702-5012.

12b. DISTRIBUTION CODE

13. ABSTRACT *(Maximum 200 Words)*

14. SUBJECT TERMS
Breast Cancer

15. NUMBER OF PAGES
52

16. PRICE CODE

17. SECURITY CLASSIFICATION OF REPORT	18. SECURITY CLASSIFICATION OF THIS PAGE	19. SECURITY CLASSIFICATION OF ABSTRACT	20. LIMITATION OF ABSTRACT
Unclassified	Unclassified	Unclassified	Unlimited

Table of Contents

Cover.....

SF 298.....

Table of Contents.....

Introduction.....5

Body.....6

Reportable Outcomes.....9

Conclusions.....9

Appendices.....10

INTRODUCTION

Hypothesis and rationale: The hypothesis of the proposal is that the cyclin-dependent kinase inhibitor p27 is regulated by androgens in both normal and neoplastic prostate. We also hypothesized that regulation occurs primarily by ubiquitin mediated degradation. This pathway affects both p27 ubiquitination (leading to degradation) and de-ubiquitination. The latter is thought to result from increased activity of de-ubiquitinating enzymes or isopeptidases, which stabilize protein targets.

Objectives and specific aims of the study:
Specific Aim 1: To determine whether testosterone (T) regulates the expression of p27 in normal and neoplastic prostate.

Specific Aim 2: To study expression of p27 in androgen-dependent (AD) and androgen-independent (AI) human prostate cancer.

Specific Aim 3: To study the role of isopeptidases in ubiquitin-proteasome dependent degradation of p27 in androgen-mediated proliferation.

Specific Aim 4: To assess the role of isopeptidases in prostate cancer cell proliferation and G1 arrest in LNCaP cells.

Statement of relevance:
p27 has been found to be one of the most important prognostic factors in human prostate carcinomas in that low levels of p27 predict a poor outcome and early recurrence. The identification of the mechanism responsible for p27 regulation in the rat model sets the stage for the development of therapeutic targets aimed at stabilizing p27 levels in human prostate cancer with the intent of slowing growth. This is particularly important in androgen insensitive tumors in which we have demonstrated a significant decrease in p27 expression, and thus a poor prognosis.

BODY

Specific Aim 1: To determine whether testosterone (T) regulates the expression of p27 in normal and neoplastic prostate. Castrated, testosterone-treated Noble rats. We have used the androgen-stimulated castrated Noble rat prostate rat model to investigate whether androgens regulate the levels of p27 in the regenerating gland. Two weeks after castration, 3-months-old rats (7 rats/condition X 3 separate experiments) were treated by I.M. T injections (6.6 mg/kg) and sacrificed at 12, 24, 48, 72, and 96 hours. Controls included 7 intact and 7 castrated untreated rats. Prior to sacrifice, rats were injected I.P. with BrdU. The prostate lobes (ventral and dorso-lateral) of each animal were harvested separately and processed for use in various assays (immunoblots, degradation and kinase assays, immunoprecipitations, quantitative real-time PCR, immunohistochemistry, hybridization *in situ*). Western blot experiments showed that (1) p27 protein levels are markedly higher in the prostate of castrated untreated rats than in that of intact animals, (2) a transient drop in p27 levels is observed after 12-24 hours of treatment followed by (3) an important increase of p27 levels at 48-72 hours.

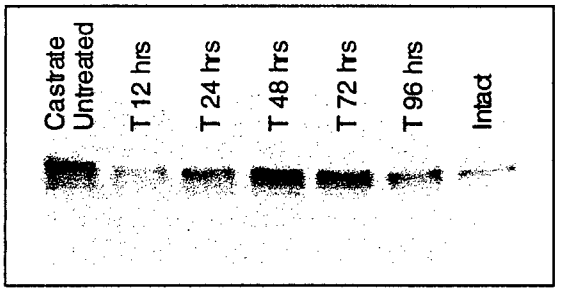

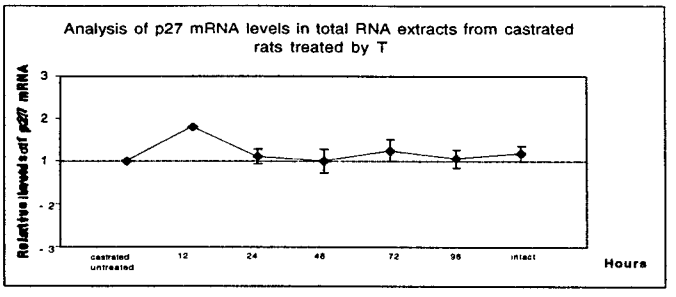

The mechanisms of regulation of p27 protein expression by androgens were investigated at both the transcriptional and the post-translational levels. Relative quantitative real-time PCR experiments using specific primers and probes for p27 show no modulation of p27 transcripts levels (normalized to β-actin) either between intact and castrated untreated rats or following T administration to castrated rats. Using *in vitro* degradation assays of recombinant histidine-tagged p27, we were able to show that p27 degradation activity by the prostate homogenates is inversely correlated with p27 protein levels. Furthermore, this degradation activity is specific for p27 since degradation of another cki, p21 (whose protein levels are highly induced by T (not shown)), is virtually unaffected by androgen replenishment.

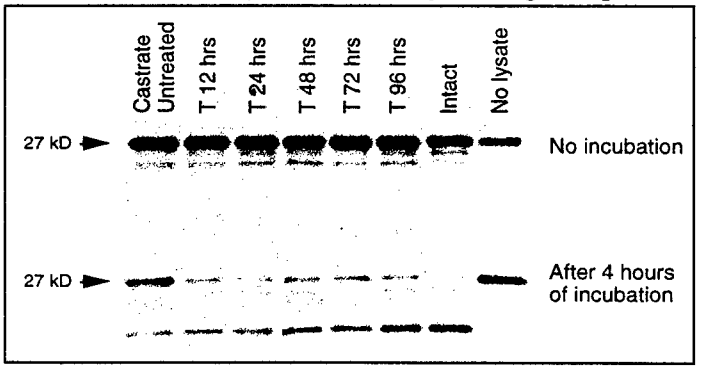

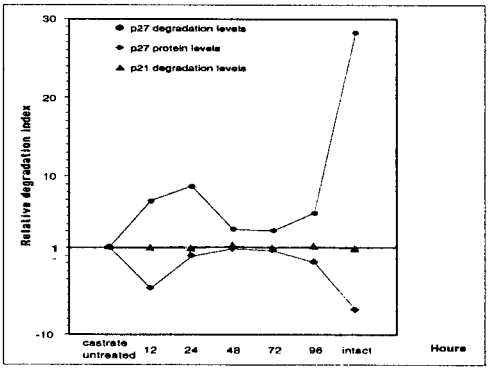

Immunohistochemical experiments yielded the following results: (1) p27 staining is detected in very few prostate epithelial cells in intact rats and BrdU labeling index is very low, (2) a strong nuclear staining is observed in most basal cells in the prostate of castrated untreated animals and BrdU staining is completely absent, (3) following T administration to castrated rats, p27 as well as BrdU are virtually undetectable at 12-24 hours, (4) at 48-72 hours, concomitantly to a marked increase in the number of BrdU+ cells, p27 is highly expressed in the majority of luminal cells.

Double immunofluorescence staining experiments for BrdU and p27 demonstrated that proliferating cells (BrdU+) are devoid of any p27 labeling and *vice versa*. In summary, we have established that changes in p27 expression which result from castration and testosterone-induced regeneration of the rat prostate are secondary to changes in p27-specific degradation rather than to transcriptional control. Furthermore, p27 expression is differentially modulated by androgens in the different cellular components of the prostate epithelium (basal *vs* luminal *vs* proliferating). Manuscript has been submitted to Molecular Endocrinology, D Waltregny et al, See Appendix.

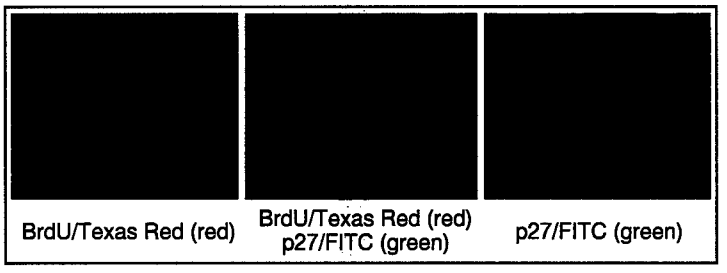

PrEC cells. We have used the normal human prostate cell line PrEC (Clonetics, San Diego) to study the regulation of p27 expression by androgens *in vitro*. We have characterized this cell line in terms of expression of high molecular weight cytokeratins (HMWCK) (+), PSA (-) and androgen receptor (-). This phenotype is consistent with that of basal epithelial type. No modulation of p27 protein expression levels were observed in these cells when grown either in the absence or in the presence of dihydrotestosterone (DHT) at various concentrations. Nevertheless, p27 was upregulated in PrECs following addition of stromal cells(PrSC cells, Clonetics)-conditioned media in the culture (PrSCs previously treated by DHT). Interestingly, a concomitant drop in p63 and HMWCK together with an increase in AR mRNA levels (protein remained undetectable) were observed, suggesting differentiation of PrECS by yet unknown molecule(s) secreted by stromal cells.

Specific Aim 2: To study expression of p27 in androgen-dependent (AD) and androgen-independent (AI) human prostate cancer. p27 expression was examined by automated immunohistochemistry in radical prostatectomies from untreated patients (n= 88; named Androgen Dependent or AD) as well as patients previously treated for at least 3 months by androgen ablation (n= 63; named Androgen Independent or AI). No correlation was found between p27 and Gleason score (p=0.13), stage (p=0.66), pre-op PSA (p=0.4) or post-op PSA (p=0.69). 50% of cases expressed p27 (>50% of cells) in AD *vs* 34% in AI (p=0.043). Results have been presented at the United States and Canadian Academy of Pathology, New Orleans, March, 2000, and an abstract is published in Laboratory Investigation (A# 545, Vol 80 (3), 2000). A manuscript is in preparation.

Specific Aim 3: To study the role of isopeptidases in ubiquitin-proteasome dependent degradation of p27 in androgen-mediated proliferation. We have evaluated the expression of Kia-190 transcripts by *in situ* hybridization in prostate, colon and breast carcinomas. Kia-190 mRNA was overexpressed in 54%, 66% and 25% of prostate, colon and breast tumors, respectively, compared with the corresponding normal tissues. These results demonstrate differential expression of Kia-190 transcripts in tumor *vs* normal tissues as well as in different epithelial tumors. A significant correlation was found between Kia-190 mRNA levels and disease stage (p=0.005) but not with Gleason score or post-op PSA.

Kia-190 mRNA expression levels by *in situ* hybridization in human cancers:

	Low	High
Prostate	50/109 (46%)	59/109 (54%)
Colon	17/51 (33%)	34/51 (66%)
Breast	23/31 (74%)	8/31 (26%)

Utilizing the antibodies we have generated, we have analysed Kia-190 protein expression in a variety of normal human tissues and tumors. Interestingly, in normal tissues Kia-190 is expressed in rapidly proliferating tissues such as colonic crypts and germinal centers.

Kia-190 protein levels by immunohistochemistry in matched prostate and colon normal and tumor samples:

	T<N	**T=N**	**T>N**
Prostate	12/105 (11%)	37/105 (35%)	56/105 (53%)
Colon	0/38 (0%)	9/38 (24%)	29/38 (76%)

Correlations bewteen Kia-190 and p27. There was no correlation between expression of Kia-190 and p27 in AD or AI cases (p=0.37). Kia-190 was found in a yeast two-hybrid screen to interact *in vivo* and *in vitro* with G3BP, a protein associated in a growth regulated manner with ras-GTPase activating protein. A manuscript is in preparation.

Specific Aim 4: To assess the role of isopeptidases in prostate cancer cell proliferation and G1 arrest in LNCaP cells. Kia-190 protein expression was studied in a variety of human cell lines by Western blot. Note absent levels of Kia-190 in [normal] PrEC prostate cells and overexpression in 3 prostate carcinoma cell lines (LNCaP, PC-3, and DU-145).

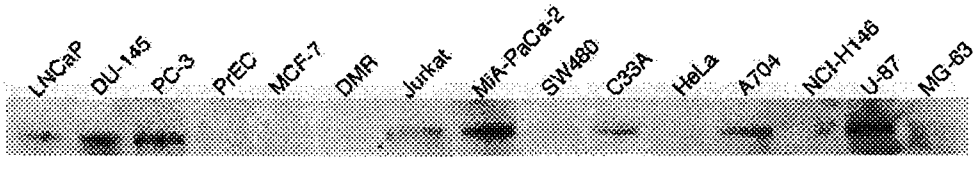

Induction of p27 by 48 hours of serum starvation was obtained in LNCaP, PC-3 and DU-145 cells. However, no concomitant change in Kia-190 protein levels was observed by Western blot (not shown). We transfected PrECs with pCR3.1/Kia-190 sense and mutated (active site cys to ala) constructs as well as pSV40-T and pCDNA3/H-rasV12 as positive controls for immortalization. Immunohistochemistry verified the successful transfection of cells. No immortalization was observed with any of the constructs. We also transfected NIH3T3 cells with pCR3.1/Kia-190 sense and mutated and pCDNA3/H-rasV12. We checked for growth in soft agar. Only clones transfected with pCDNA3/H-rasV12 (with or without Kia-190) were able to grow in soft agar.

CONCLUSION

Overview of the work accomplished: During the first year of this grant, we have actively investigated the mechanisms of androgen-mediated p27 regulation. We have established that expression of p27 in the 'castrated-regenerating' Noble rat prostate model is regulated primarily by ubiquitin-mediated degradation. Castration blocks the elevated p27 degradation activity characteristic of intact rat prostates, leading to increased expression of p27. During testosterone-induced regeneration, p27 degradation inversely correlates with p27 expression. Because the focus of the proposal is androgen regulation of p27, p27 was evaluated in androgen naïve *vs* tumors treated with androgen ablation. Androgen ablation results in a significantly higher numbers of tumors expressing low levels of p27 suggesting a selection for more aggressive p27 negative tumors with this therapeutic modality. Finally, we suggested the possibility that de-ubiquitinating enzymes may be responsible for stabilizing p27 levels in prostate cancer. The isopeptidase KIA190 was studied in human tumors as well as prostate basal cells grown in culture and human prostate cancer cell lines utilizing a novel antibody we generated. There was overexpression of KIA190 in prostate tumors and tumor cell lines compared with normal tissues. Although this isopeptidase seemed to be the most promising candidate for p27 regulation based on preliminary data, no correlation between KIA190 and p27 was found. KIA190 did not transform normal prostate cells when transfected.

Conclusion: Low levels of p27 predict a poor outcome and early recurrence in human prostate carcinomas. The identification of the mechanism responsible for p27 regulation in castrated-regenerating prostate sets the stage for the development of therapeutic targets aimed at stabilizing p27 levels in human prostate cancer with the intent of slowing growth. This is particularly important in androgen insensitive tumors in which we have demonstrated a significant decrease in p27 expression, and thus a poor prognosis. Recently, the ubiquitin ligase responsible for targeting p27 for degradation has been identified. In collaboration with Michele Pagano (NYU), we characterized antibodies to this ligase, named skp2.

Future Direction: We plan to submit a phase II proposal to investigate whether skp2 is the direct target of androgens in the regulation of p27.

Reportable Outcomes: As a result of the research accomplished, we have 3 manuscripts in preparation: 1) Regulaton of p27 in the castrated-regenerating Noble rat prostate model; 2) Downregulation of p27 in adenocarcinoma of prostate after androgen ablation (Abstract published- Lab Invest, A# 545, 80(3), 2000); 3) Overexpression of the isopeptidase KIA190 in human prostate cancer. The castrated-regenerating Noble rat prostate model we utilized is an excellent model to study protein regulation affected by androgens. Obtaining this DOD award has been instrumental in the establishment of a strong program of prostate cancer research in our laboratory and had been key to my promotion to associate professor at Harvard Medical School as well as to my recruitment to the Dana-Farber Cancer Institute.

APPENDICES

1. Waltregny D, et al. Androgen-driven prostate epithelial cell proliferation and differentiation in vivo involve the regulation of $p27^{kip1}$ through its proteasome-mediated degradation. (Submitted to Molecular Endocrinology)

Androgen-driven prostate epithelial cell proliferation and differentiation *in vivo* involve the regulation of $p27^{KIP1}$ through its proteasome-mediated degradation

David Waltregny[1], Irwin Leav[3], Sabina Signoretti[1,2], Peggy Soung[1], Douglas Lin[1], Frederick Merk[3], Jason Y. Adams[2], Nandita Bhattacharya[1], Nicola Cirenei[1] and Massimo Loda[1,2]

Department of Adult Oncology[1], Dana-Farber Cancer Institute, and Department of Pathology[2], Brigham and Women's Hospital, Harvard Medical School, Boston, 02115 Massachusetts

Department of Pathology[3], Medicine and Veterinary School, Tufts University, Boston, 02111 Massachusetts

Running title: androgen regulation of $p27^{KIP1}$ in the regenerating prostate

Key words: cell cycle, regenerating prostate, rat model, $p27^{KIP1}$, androgens, ubiquitin-proteasome-mediated degradation, real-time PCR

Address for correspondence and reprint requests:
Massimo Loda, M.D.
Department of Adult Oncology, Dana Building 740B,
Dana-Farber Cancer Institute,
44, Binney Street,
Boston, MA 02115
☎: (617) 632 4001
Fax: (617) 632 4005
Email: Massimo_Loda@dfci.harvard.edu

ABSTRACT

Androgens control both growth and differentiation of the normal prostate gland. However, the mechanisms by which androgens act upon the cell cycle machinery to regulate these two fundamental processes are largely unknown. The cyclin-dependent kinase (cdk) inhibitor $p27^{KIP1}$ is a negative cell cycle regulator involved in differentiation-associated growth arrest. Here, we investigate the role and regulation of $p27^{KIP1}$ in the testosterone (T)-stimulated regeneration of the ventral prostate (VP) of castrated rats.

Continuous T administration to castrated rats triggered epithelial cell proliferation, which peaked at 72 hours, and then declined despite further treatment. Castration-induced atrophy of the VP was associated with a significant increase in $p27^{KIP1}$ expression as compared with the VP of intact animals. Twelve hours after the initiation of T treatment, total $p27^{KIP1}$ levels as well as its fraction bound to cdk2, its main target, significantly dropped in the VP of castrated rats. Thereafter, concomitantly to the induction of epithelial cell proliferation, the glandular morphology of VP was progressively restored at 48-96 hours of T treatment. During this period of the regenerative process, whereas both proliferating basal and secretory epithelial cells did not express $p27^{KIP1}$, the protein was selectively upregulated in the (non-proliferating) secretory epithelial compartment. This upregulation of $p27^{KIP1}$ expression was coincident with an increase in its association with, and presumably inhibition of, cdk2. At each time point of T treatment, $p27^{KIP1}$ abundance in the VP was inversely correlated with the level of its proteasome-dependent degradation activity whereas only slight changes in the amount of $p27^{KIP1}$ transcripts were detected.

Taken together, our data indicate that $p27^{KIP1}$ may mediate androgen-driven proliferation and differentiation signals in the normal prostate epithelial cells through regulation of its proteasome-mediated degradation.

INTRODUCTION

Cell proliferation and differentiation are controlled by extracellular signals that impinge upon the cell cycle machinery and modulate the expression/activity of key cell cycle regulators. In the normal prostate gland, these two fundamental processes are regulated to a large extent by androgens (1). Like its human counterpart, the epithelial compartment of the rat prostate is composed of two types of cells: basal and secretory cells. Secretory cells compose approximately 85% of the total cells in the ventral prostate (VP) of a sexually mature male rat. Basal cells are numerically less abundant and their function is still poorly understood, although they are believed to be precursors of secretory cells (2, 3). Following castration, the rat prostate rapidly involutes as a result of a major loss of secretory cells (60%-70% within 7 days of androgen deprivation), which chronically require physiological levels of androgens for their maintenance (3, 4). Testosterone stimulation can dramatically accelerate the proliferation rate of prostate epithelial cells in a sexually immature rat, yet once the organ has attained adult size additional androgen has little influence on proliferation (5). Likewise, sustained androgen administration to mature castrated rats can trigger the regrowth of the prostate gland, which will eventually return to its original size (5-7). This regenerative process is timely regulated since proliferation rates decline to the baseline levels found in intact animals despite further androgen treatment (6, 8). Concomitantly with their mitogenic activity, androgens induce histological and biochemical changes characteristic of glandular differentiation in the prostate of castrated rats (5-7, 9, 10). For example, testosterone replenishment in castrated rats results in the reconstitution of the normal secretory cell compartment simultaneous with a significant reduction in VP expression levels of basal cell-associated cytokeratins (7, 9). In addition, the mRNA levels of the C3 gene, which encodes for a major subunit of a prostate secretory protein (prostatic steroid-binding protein) exclusively expressed in secretory cells, are dramatically induced in the regenerating VP of castrated rats (11, 12).

The regulation of mammalian cell proliferation by growth stimulatory and growth inhibitory extracellular signals occurs during the first gap (G1) phase of the cell cycle. The enzymes that regulate G1 phase progression include the cyclin-dependent kinases cdk4 and cdk6, which can be activated through their association with D-type cyclins, and cdk2, which forms active complexes with cyclins E and A [for reviews, see references (13-15)]. The activity of these cdk/cyclin complexes is negatively regulated by cyclin-dependent kinase inhibitors (ckis) which belong to two known families (16). The INK4A family comprises $p16^{INK4A}$, $p15^{INK4B}$, $p18^{INK4C}$ and $p19^{INK4D}$, which bind to and specifically inhibit cdk4 and cdk6. The CIP/KIP family includes $p21^{WAF1}$, $p27^{KIP1}$ and $p57^{KIP2}$, which preferentially target cdk2 complexes (16-18).

The cki $p27^{KIP1}$ was initially identified as an inhibitor of cdk2/cyclin E complex activity in transforming growth factor-ß treated or contact inhibited mink lung epithelial cells (19) and it was found to induce cell cycle arrest when overexpressed in cultured cells (20, 21). $p27^{KIP1}$ has since been shown to play a pivotal role in mediating G1 arrest in some normal and neoplastic cells in response to a variety of antiproliferative signals, including growth in suspension (22), cAMP agonists (23), IFN-ß (24) and -γ (25), IL-6 (26) and rapamycin (27). In contrast to $p21^{WAF1}$, $p27^{KIP1}$ expression is highest in quiescent cells (28, 29) and declines as cells are stimulated to reenter the cell cycle (27, 28). $p27^{KIP1}$ abundance is regulated primarily at the posttranslational level. Once activated, cdk2/cyclin E complexes phosphorylate $p27^{KIP1}$ at Threonine-187 (30-33), thereby signaling for its degradation by the ubiquitin-proteasome system through the ubiquitin-ligase SCFSkp2 complex (34, 35). Hence, maximum degradation of $p27^{KIP1}$ by the ubiquitin-proteasome pathway is detected in extracts prepared from cells in S-phase (36). Accumulation of $p27^{KIP1}$ can however also be regulated by other mechanisms, including transcriptional (26, 37-39) and translational control (40, 41).

Several lines of evidence from studies in $p27^{KIP1}$ knock-out mice indicate a direct involvement of $p27^{KIP1}$ in differentiation-associated cell cycle arrest. Homozygous $p27^{KIP1}$-deficient female mice display infertility with both impaired release of eggs during the estrus cycle and deficient implantation of embryos (42-44). In this instance, the absence of $p27^{KIP1}$ prevents the coupling of differentiation with growth arrest in granulosa cells in response to luteinizing hormone (45, 46). Other studies using $p27^{KIP1-/-}$ mice have highlighted an important role for this protein in regulating the differentiation of oligodendrocytes (47) and osteoblasts (48). In addition, $p27^{KIP1}$ expression increases during the differentiation of various normal and neoplastic cell types, both *in vivo* and *in vitro* (49). For example, treatment of LNCaP human prostate cancer cells with IL-6 (50) or the flavanoid antioxidant silibinin (51) results in increased $p27^{KIP1}$ expression associated with G1 arrest and neuroendocrine differentiation.

Prior data have suggested that androgens regulate the expression of $p27^{KIP1}$ in both normal and neoplastic prostate epithelial cells, and that $p27^{KIP1}$ levels may mediate the androgen-driven proliferative and differentiation signals in such cells (7, 52-55). However, the mechanisms by which androgens modulate the expression of $p27^{KIP1}$ are unknown. Testosterone-induced regeneration of the castrated rat VP follows a highly reproducible time course, thus making this system an excellent model for scrutinizing the androgen-mediated regulation of proteins involved in the cell cycle. In this study, we have used this model in order to investigate the regulation of $p27^{KIP1}$ by testosterone. We herein provide convincing evidence that in this system (1) $p27^{KIP1}$ likely plays an important role in the control of testosterone-stimulated proliferation and differentiation of normal prostate epithelial cells and (2) testosterone regulates the expression of $p27^{KIP1}$ mainly through modulation of its specific degradation by the ubiquitin-proteasome proteolytic system.

MATERIALS AND METHODS

Animals and Tissues

All animals were maintained in accordance with the NIH Guide for the Care and Use of Laboratory Animals, and the specific protocol used in this study was approved by the Dana-Farber Cancer Institute Animal Care and Use Committee. Twelve week-old male Noble rats were purchased from Charles River Laboratories (Boston, MA). Fourteen days after surgical castration, rats were injected with 6.6 mg/kg Testosterone (T) Propionate (Sigma Chemical Co., St. Louis, MO) in tocopherol-stripped corn oil (ICN Biomedicals, Inc., Aurora, OH) im, once a day, for 4 days. At 0, 12, 24, 48, 72 and 96 hours after the beginning of T injections, animals (seven rats per time point) were injected ip with 5 ml of phosphate buffered saline containing 10 mM BrdU (Boehringer Mannheim GmbH, Mannheim, Germany) and sacrificed 30 minutes later by CO_2 asphyxiation. The ventral prostate (VP) was then harvested, freed of fat, and 2 thirds of each VP were immediately flash-frozen in liquid nitrogen and then stored at –80°C for subsequent RNA and protein isolation. The remaining third of each VP was fixed in 10% phosphate buffered formalin overnight, dehydrated in graded alcohols, and paraffin embedded for immunohistochemical procedures. Seven non-castrated untreated age-matched male rats were also included as control animals.

Protein and RNA Extraction

The frozen VP specimens from each group of seven rats were randomly pooled in two separate sample duplicates containing 3 and 4 VP specimens, each. All the experiments described in this study were performed with both sets of pooled samples and yielded reproducible results (data not shown). The pooled frozen VP samples were homogenized by pulverization using a Mikro-Dismembrator S (Braun Biotech., Melsungen, Germany) to generate a tissue powder that was

immediately processed for protein and RNA extraction. Total RNA was extracted from 10-20 mg of each tissue homogenate by using the RNeasy mini kit (Qiagen, Inc., Valencia, CA), according to the manufacturer's protocol. The remaining tissue powder was lysed in 3.5 vol/wt of lysis buffer [10% sucrose, 1% Nonidet P-40, 20 mM Tris (pH 8.0), 137 mM NaCl, 10% glycerol, 2 mM EDTA, 10 mM NaF, 1 mM Na_3VO_4] containing phenylmethylsulfonyl fluoride (1 mM), soybean trypsin inhibitor (10 μg/ml), leupeptin (1 μg/ml) and aprotinin (1 μg/ml). Protein lysates were placed in ice for 30 minutes, vortexed every 10 minutes and then cleared by centrifugation at 12,000 X *g* for 20 minutes at 4°C. The supernatants were retrieved and frozen at –80°C until use in immunoblot, co-immunoprecipitation, and degradation assays. The protein concentration was measured using the Bio-Rad protein assay kit (Bio-Rad Laboratories, Hercules, CA).

Western Blot Analysis

Protein lysates (100 μg from each sample) were resolved by size on 12% or 16% SDS-polyacrylamide gels and transferred onto nitrocellulose membranes (Protran®, Schleicher & Schuell, Keene, NH), which were stained with Ponceau S (Sigma Chemical Company, St. Louis, MO) to examine the equal protein sample loading and transferring (data not shown). The membranes were blocked with 5% non-fat dry milk in Tris-buffered saline (20 mM Tris base [pH 7.6], 150 mM NaCl) containing 0.1% Tween-20 (TBS-T), and probed with the following antibodies: anti-cdk2 (M2) (0.4 μg/ml), anti-cdk4 (C-22) (0.4 μg/ml), anti-cdk6 (C-21) (0.4 μg/ml), anti-cyclin E (M-20) (0.4 μg/ml), anti-$p21^{WAF1}$ (C-19) (0.4 μg/ml) (Santa-Cruz Biotechnology, Inc., Santa Cruz, CA), anti-androgen receptor (AR) (PG-21) (1.5 μg/ml) (Upstate Biotechnology, Inc., Lake Placid, NY), anti-cyclin D1 (CC12) (0.8 μg/ml) (Calbiochem® Oncogene, Cambridge, MA), and anti-$p27^{KIP1}$ antibodies (0.1 μg/ml) (Transduction Laboratories, Inc., Lexington, KY). After washing in TBS-T, membranes were incubated with horseradish peroxidase (HRP)-conjugated

secondary antibodies (Bio-Rad Laboratories, Hercules, CA) and developed using an enhanced chemiluminescence detection system (ECL detection kit; Amersham Corp., Arlington Heights, IL) according to the instructions of the manufacturer. Membranes were exposed to Kodak X-Omat AR films. The immunoblots were quantitated by densitometric analysis using the ImageQuant™ software (Molecular Dynamics, Inc., Sunnyvale, CA).

Co-Immunoprecipitation Assay

In order to study the association of $p27^{KIP1}$ with cdk2/cyclin complexes, lysates containing 500μg of total proteins normalized to a 1 ml volume in lysis buffer were precleared by incubation with 100 μl of a 1:1 vol/vol slurry of protein A-sepharose beads (Sigma Chemical Company, St. Louis, MO) for 45 min on a rotator at 4°C. Protein complexes were immunoprecipitated from the precleared lysates by addition of 1.5 μg of anti-cdk2 antibodies overnight at 4°C with constant rotation, followed by the addition of 50 μl of a 50% slurry of beads for 45 min at 4°C with mild agitation. After 3 washes with 1ml cold lysis buffer, pelleted beads were quenched in 20 μl of 2X Laemmli sample buffer and boiled. The mixtures were spun down at 10,000 X *g* for 30 seconds and 20 μl of each supernatant were retrieved and analyzed by immunoblot using anti-$p27^{KIP1}$ antibody as described above. The filters were subsequently stripped and reprobed with an anti-cdk2 antibody to examine the amount of immunoprecipitated cdk2 in the different samples tested. Immunoprecipitations with 1.5 μg of rabbit immunoglobulins G (IgG) (Vector Laboratories, Burlingame, CA) instead of anti-cdk2 antibodies were used as negative control experiments.

Degradation Assay

Degradation assay experiments were performed as previously described (36, 56, 57) with minor modifications. 300 ng of human hexahistidine(his_6)-tagged $p27^{KIP1}$ and $p21^{WAF1}$ proteins (bacterially

expressed and purified as in reference (36)) were incubated at 37°C for 0, 1, 4 and 15 hours in 60 µl of degradation mix containing 100 µg of protein homogenates, 50 mM Tris-HCl (pH 8.0), 5 mM $MgCl_2$, 1 mM dithiothreitol, 2mM ATP, 60 µg/ml creatine phosphokinase, 10 mM creatine phosphate, and 5 µM ubiquitin. The reactions were carried out in a PCR instrument and stopped at the different time points by addition of 2X Laemmli sample buffer. The degradation of his_6-tagged $p27^{KIP1}$ and $p21^{WAF1}$ proteins by the rat VP protein lysates was analyzed by immunoblotting with an anti-histidine monoclonal antibody (0.1 µg/ml) (Qiagen, Inc., Valencia, CA), as detailed above. To ensure that endogenous $p27^{KIP1}$ present in the VP lysates was not significantly competing for proteasome degradation with his_6-tagged $p27^{KIP1}$, we had previously checked by Western blot using an anti-$p27^{KIP1}$ antibody that the amount of exogenous $p27^{KIP1}$ added to the degradation mixtures was in large excess to that of endogenous $p27^{KIP1}$ (data not shown). Control degradation experiments included the omission of the his_6-tagged protein as well as the omission of the lysate from the degradation mix. In order to demonstrate that $p27^{KIP1}$ degradation activity was dependent on the proteasome proteolytic activity of the lysates, degradation assays were performed, in which either the proteasome inhibitor MG-132 (Carbobenzoxyl-L-leucyl-L-leucyl-L-leucinal, Calbiochem-Novabiochem Corp., La Jolla, CA) dissolved in dimethylsulfoxyde (DMSO) (100 µM final concentration) or DMSO alone was added to the degradation mixture. Quantification of degradation activity was done by densitometric analysis of the bands of slowest electrophoretic migration, *in extenso* the bands at ±22kDa and ±28kDa corresponding to undegraded his_6-tagged $p21^{WAF1}$ and $p27^{KIP1}$ proteins, respectively. Relative degradation activity of the samples at each time point following T injections was then calculated by dividing the densitometric volume of the band obtained without incubation (0 hour) by the one obtained after 4 hours of incubation in the degradation mix.

Real-Time Reverse Transcription Polymerase Chain Reaction (Taqman® RT-PCR)

Reverse Transcription. For cDNA synthesis, 1 μg of total RNA was reverse-transcribed in a 20 μl reaction mixture containing 250 μM of each dNTP, 20 U of RNase inhibitor, 50 U of MuLV Reverse Transcriptase (RT), 2.5 μM Random Hexamers, and 1X buffer (1.5 mM MgCl2) (all reagents purchased from PE Applied Biosystems, Foster City, CA). The reaction mix was incubated at 42°C for 45 min and then denatured at 99°C for 5 min. Reactions not containing the RT or omitting the target RNA were used as controls.

Primers and Probes. Specific primers and probes for rat $p27^{KIP1}$ and $p21^{WAF1}$ genes (Table 1) were designed from sequences available in the GenBank database, using the Primer Express 1.0 Software (PE Applied Biosystems, Foster City, CA). The housekeeping glyceraldehyde-3-phosphate dehydrogenase (GAPDH) gene (Taqman® rodent GAPDH control reagents kit, PE Applied Biosystems, Foster City, CA) was used as endogenous control to normalize the amount of $p27^{KIP1}$ and $p21^{WAF1}$ transcripts in each reaction. The choice of this reference gene was guided by results from a previous study showing that GAPDH mRNA levels were not significantly altered in the regenerating prostate of castrated rats treated by T (12). All sets of primers and probe were selected to work under identical cycling conditions. cDNA amplification products with the different primer pairs had been previously checked to yield a single band of the expected size after electrophoretic migration in a 2% agarose gel stained with ethidium bromide (data not shown). Probes were synthesized by PE Applied Biosystems.

Real-Time PCR. Taqman® PCR was performed on the cDNA samples using an ABI PRISM 7700 Sequence Detector (PE Applied Biosystems, Foster City, CA). The Taqman® PCR Core Reagent kit (PE Applied Biosystems) was used according to the manufacturer's directions with the following modifications: dUTP was replaced by dTTP at the same concentration, and incubation with

AmpErase was omitted. For each sample tested, PCR reaction was carried out in a 50 µl volume containing 1 µl of cDNA reaction (equivalent to 50 ng of template RNA) and 2.5 U of AmpliTaq Gold® (PE Applied Biosystems, Foster City, CA). Oligonucleotide primers and fluorogenic probes were added to a final concentration of 100 nM each. After activation of AmpliTaq Gold® for 10 min at 94°C, amplification step consisted of 60 cycles of 94°C for 45 sec, 58°C for 45 sec, and 64°C for 1 min.

In each experiment, 7 additional reactions with serial dilutions (500X magnitude) of intact VP cDNA as template were performed with each set of primers and probe in the same 96 well plate to generate standard curves relating the threshold cycle (C_T) to the log input amount of template. All samples were run in triplicates. The relative amounts of $p27^{KIP1}$ and $p21^{WAF1}$ transcripts in each sample were determined using the standard curve method and were normalized to GAPDH mRNA expression levels, as described in detail in ABI PRISM Sequence Detection System User Bulletin #2 (PE Applied Biosystems) and elsewhere (58).

Immunohistochemistry and Immunofluorescence

Antibodies and immunodetection of $p27^{KIP1}$ and BrdU. Immunostaining experiments for $p27^{KIP1}$ and BrdU were performed in all paraffin-embedded VP tissue specimens with anti-$p27^{KIP1}$ (Transduction Laboratories, Inc., Lexington, KY) and anti-BrdU monoclonal antibodies (Becton Dickinson, Mansfield, MA), respectively. Double immunofluorescence staining for $p27^{KIP1}$ and BrdU was performed in the paraffin-embedded VP specimens from 7 castrated rats that had been sacrificed at 72 hours of T treatment.

Five µm sections were deparaffinized in xylene, then rehydrated and subjected to microwaving in 10 mM citrate buffer, pH 6.0 (BioGenex, San Ramon, CA) in a 750W oven for 15 minutes. Slides were allowed to cool at room temperature (RT) for 30 min. Immunohistochemistry

was performed by an automated processor (Optimax Plus 2.0 bc, BioGenex, San Ramon, CA). After quenching of the endogenous peroxidase activity with 3% hydrogen peroxide in methanol for 10 minutes, slides were incubated for 10 minutes with a buffered casein solution (Power Block Reagent, BioGenex, San Ramon, CA) to block the nonspecific binding sites. Antibodies (anti-$p27^{KIP1}$, 1:3000 dilution; anti-BrdU, 1:100 dilution) were applied at RT for 2 hours in the automated stainer. Detection steps were performed by the instrument utilizing the MultiLink-HRP kit (BioGenex, San Ramon, CA). Standardized development times with the chromogenic substrate [3,3' – diaminobenzidine tetrahydrochloride (DAB) (for anti-$p27^{KIP1}$ staining) ± nickel chloride (DAB-NC) (for anti-BrdU staining)] allowed accurate comparison of all samples. Sections were counterstained with hematoxylin, rehydrated and mounted for microscopic examination.

For double immunofluorescence staining experiments, antigen retrieval and blocking steps were performed as described above. Anti-$p27^{KIP1}$ antibody (dilution 1:100) was applied at RT for 1 hour. Sections were then incubated with secondary biotinylated antibody (MultiLink, BioGenex, San Ramon, CA), followed by detection with fluorescein isothiocyanate (FITC)-conjugated streptavidin (Vector Laboratories, Burlingame, CA). Sections were then blocked with, successively, FITC-conjugated anti-mouse immunoglobulin antibody (Vector Laboratories, Burlingame, CA), a blocking solution (Power Block, BioGenex, San Ramon, CA), avidin, and biotin (both from BioGenex, San Ramon, CA), for 10 minutes each. Subsequently, anti-BrdU antibody (dilution 1:10) was applied for 1 hour at RT. Then, sections were incubated with a secondary antibody (MultiLink, BioGenex, San Ramon, CA) and detection was performed by addition of Texas Red-conjugated streptavidin (Vector Laboratories, Burlingame, CA). Slides were mounted with an anti-fading fluorescent medium for microscopic examination and photomicrography under an Olympus BX50 microscope equipped with appropriate filters.

Substitution of the primary antibodies with PBS served as negative staining control. For $p27^{KIP1}$, strong immunoreactivity in small lymphocytes, which invariably infiltrated the prostate stroma, was used as an internal positive control.

Evaluation of immunohistochemical staining. The percentage of BrdU-positive epithelial cells in each VP was calculated by dividing the number of epithelial cells with BrdU-positive nucleus by the total number of epithelial cells counted (≈1000 cells). BrdU counts were done separately in basal cells and secretory cells from the VP of castrated rats treated by T for 72 hours. Scoring of $p27^{KIP1}$ immunostaining was done according to the percentage of epithelial cells (≈500 cells counted) exhibiting detectable nuclear anti-$p27^{KIP1}$ reactivity, as previously described (56, 59). $p27^{KIP1}$ scores were determined in the basal and secretory cell subsets separately in all VP specimens. All scoring values are expressed as the mean ± standard error for each group of 7 rats.

Statistical analysis

The paired t-test was used to assess whether there were significant differences in $p27^{KIP1}$ expression (percentage of positive cells) between basal and secretory cells within the same VP specimen at each time point of T treatment. The same test was performed to examine the statistical significance of differences in the percentages of BrdU-positive cells between the basal and secretory compartments in the VP of rats treated by T for 72 hours. The unpaired t-test was used to determine whether there were significant differences in the percentages of $p27^{KIP1}$-positive basal or secretory cells between rats treated by T for different times. The tests were two-tailed and $P<0.05$ was considered statistically significant. The analyses were performed with a statistics software package (Statview 4.02, Abacus Concepts Inc., Berkeley, CA).

RESULTS

Epithelial cell proliferation in the VP of castrated rats following androgen treatment

As expected, T administration to the castrated rats caused a dramatic regrowth of their VP, which returned to a size almost comparable to that of age-matched non castrated rats after 4 days of treatment (data not shown). *In situ*, proliferating epithelial cells were recognized by immunohistochemical detection of BrdU. Figure 1A shows representative examples of anti-BrdU immunostaining of VP epithelial cells at each time point of T treatment as well as those from intact animals. Virtually no detectable anti-BrdU nuclear staining was identified in epithelial cells from untreated castrated or intact rats. The induction of cell proliferation became apparent 48 hours after the initiation of T treatment and BrdU incorporation was detected in both basal and secretory cell subsets (Figure 1A, inset). The proportion of DNA-synthesizing basal and secretory cells reached a peak at 72 hours (11.7%±0.2%), and then declined in both cell types despite further androgen administration (Figure 1B). Interestingly, at peak proliferation rate, the percentage of BrdU-positive basal cells (22.9%±0.6%) was almost 2.5 times higher than the percentage of BrdU-positive secretory cells (9.2%±0.5%) (paired t-test, $P<0.0001$).

Expression of G1-related cdks, cyclins and ckis in the VP of androgen-replenished castrated rats

In order to understand the relationship between androgen stimulus and the proliferation/differentiation response of regenerating VPs, we next investigated the temporal changes in expression levels of $p27^{KIP1}$ and other key regulators involved in the G1 phase progression of the cell cycle. Changes in androgen receptor (AR) expression were also examined. Western blot analysis of AR, cdk2, cdk4, cdk6, cyclin D1, cyclin E, $p21^{WAF1}$ and $p27^{KIP1}$ expression

was performed by using total VP protein lysates from rats sacrificed at each time point of androgen treatment (Figure 2).

Although the expression of AR was dramatically induced as early as 12 hours after the initiation of T treatment, the levels of cdks and their associated cyclins remained unchanged at this time point. The expression levels of these cell cycle proteins gradually increased at 24 hours of treatment and peaked during the next 3 days. $p21^{WAF1}$ protein was virtually undetectable in the VP of untreated castrated rats and during the first 24 hours of T replenishment. Thereafter, its expression gradually increased. The highest level of $p21^{WAF1}$ expression was detected in the VP of intact rats.

$p27^{KIP1}$ expression levels followed more complex temporal changes. The protein levels were highest in the VP of untreated castrated rats. T administration induced an early (12 hours) substantial decrease in $p27^{KIP1}$ expression. Subsequently, $p27^{KIP1}$ levels increased and peaked at 72 hours (concomitantly with maximal proliferation rate) and decreased again at 96 hours of treatment. The protein abundance was the lowest in the VP of intact animals.

In situ expression of $p27^{KIP1}$ in the regenerating VP of castrated rats

Since our Western blot experiments were performed with the use of total protein extracts, it was possible that the changes in $p27^{KIP1}$ expression levels detected with this technique may not reflect those that take place in the epithelial cells. Thus, to rule out this potential bias as well as to assess $p27^{KIP1}$ expression in the two subsets of VP epithelial cells, we used immunohistochemistry. Figure 3A shows representative examples of anti-$p27^{KIP1}$ immunostaining in VP glands during the first 96 hours of T administration to castrated rats as well as in the VP of intact animals. $p27^{KIP1}$ expression was scored separately in the basal and secretory cells according to the percentage of positive cells (Figure 3B).

$p27^{KIP1}$ immunoreactivity in the epithelial cells was mainly nuclear (Figure 3A). Overall, temporal changes in $p27^{KIP1}$ expression levels were similar in basal and secretory cell compartments and strictly paralleled those detected by Western blot in the corresponding total protein extracts (compare Figure 3B and Figure 2).

Comparison of $p27^{KIP1}$ expression levels in epithelial cells between each time point of T treatment. The percentages of $p27^{KIP1}$-expressing epithelial cells were high in the VP of untreated castrated rats and, after 12 and 24 hours of T treatment, fell significantly in secretory (unpaired t-test, P=0.03) and basal cells (unpaired t-test, P=0.05), respectively. Subsequently, $p27^{KIP1}$ expression levels increased in both cell types and peaked at 72 hours of treatment. However, this increase in $p27^{KIP1}$ levels was significant only in the secretory cell subset (unpaired t-test, P=0.2 and P<0.0001 for basal and secretory cells, respectively). $p27^{KIP1}$ levels then slightly dropped in both subsets of cells at 96 hours of treatment (unpaired t-test, NS). The lowest level of $p27^{KIP1}$ expression was found in the VP epithelial cells of intact animals.

Comparison of $p27^{KIP1}$ expression levels between basal and secretory cells at each time point of T treatment. In the VP of untreated castrated rats, a significantly higher percentage of $p27^{KIP1}$-positive cells was observed in the basal compartment (64.7%±12.8%) than in the secretory one (45.6%±9.3%) (paired t-test, P=0.005) (Figure 3B). After 24 hours of T treatment, the level of $p27^{KIP1}$ expression was almost similar in both cell types (paired t-test, NS). Subsequently, at 48-96 hours of treatment, $p27^{KIP1}$ expression levels were significantly higher in secretory than in basal cells (paired t-test, P<0.05). Also, a significant difference in the percentages of basal (4.6%±2%) and secretory (7%±2.8%) $p27^{KIP1}$-positive cells was observed in the VP of intact animals (paired t-test, P<0.05).

Thus, both our immunohistochemical and immunoblot analyses of $p27^{KIP1}$ expression yielded similar results, showing an early and significant T-induced downregulation of $p27^{KIP1}$ in the regenerating VP of castrated rats. In addition, our data unexpectedly indicated that $p27^{KIP1}$ levels were high in the regenerating VP at peak proliferation rate (72 hours). Indeed, this observation was in apparent contradiction with the fact that $p27^{KIP1}$ expression is known be downregulated in proliferating cells (36).

To understand this paradox, we performed double immunostaining experiments for BrdU and $p27^{KIP1}$ using VP tissue sections from animals sacrificed at 72 hours of T treatment. Remarkably, all epithelial cells in S-phase (BrdU-positive) exhibited no detectable $p27^{KIP1}$ expression (Figure 4 A-C). Thus, during the proliferation phase, two main subsets of epithelial cells could be distinguished: cells in S phase (BrdU positive/ $p27^{KIP1}$ negative) and cells likely to be arrested in G1 phase (BrdU negative/ $p27^{KIP1}$ positive). In addition, a small proportion of basal and secretory cells were double negative for both antibodies.

Association of $p27^{KIP1}$ with cdk2/cyclin complexes in the regenerating VP of castrated rats

In order to further substantiate our results, we determined whether the increased levels of $p27^{KIP1}$ expression detected at 72 hours of T replenishment would translate into an increased association of $p27^{KIP1}$ with cdk2. We performed co-immunoprecipitation experiments in which cdk2 was pulled down from the VP protein lysates at the different time points of T treatment. The immunoprecipitates were subjected to SDS-PAGE and transferred to nitrocellulose membranes that were blotted with an anti-$p27^{KIP1}$ antibody (Figure 5A).

Temporal changes in the association of $p27^{KIP1}$ with cdk2 matched those in endogenous $p27^{KIP1}$ protein expression (compare Figure 5A and Figure 2). Indeed, as compared to the VP of untreated castrated rats, the amount of cdk2/$p27^{KIP1}$ complexes was substantially decreased and

almost undetectable in the VP of castrated rats treated by T for 12 or 24 hours. The abundance of $p27^{KIP1}$ bound to cdk2 increased significantly at 48 hours of T treatment, peaked at 72 hours, and then declined at 96 hours despite further T treatment. The lowest amount of cdk2 bound-$p27^{KIP1}$ was found in the VP of intact animals. The increased association of $p27^{KIP1}$ with cdk2 at 48-96 hours of T treatment was not merely due to an increased amount of cdk2 protein in the lysates since the abundance of immunoprecipitated cdk2 was similar in all samples (Figure 5B).

Evidence for androgen regulation of $p27^{KIP1}$ expression by degradation *via* the ubiquitin-proteasome pathway

We next searched for the mechanisms responsible for the regulation of $p27^{KIP1}$ expression by T. We first tested for levels of $p27^{KIP1}$ ubiquitin-proteasome-mediated degradation activity in the different VP lysates by using a previously described assay (36, 56, 57) in which purified recombinant his_6-tagged $p27^{KIP1}$ serves as a substrate to the lysates. Kinetic profiles of $p27^{KIP1}$ degradation obtained by using the samples from each time point of T treatment clearly showed that VP protein lysates were able to degrade exogenous $p27^{KIP1}$ and that this ability to degrade the protein was modulated in time, as prostates were replenished with T (Figure 6A). $p27^{KIP1}$ was degraded in a proteasome-dependent manner since the addition of a specific proteasome inhibitor (MG-132) to the VP protein lysates completely nullified $p27^{KIP1}$ degradation (Figure 6C).

In order to measure $p27^{KIP1}$ degradation activity levels in the different samples and to correlate these levels with the expression levels of the endogenous protein in the corresponding samples, the relative amounts of undegraded his_6-$p27^{KIP1}$ after 0 and 4 hours of incubation in presence of the lysates were analyzed by Western blotting and quantified by densitometry. $p27^{KIP1}$ abundance was inversely correlated with the level of degradation activity for the protein during the

course of T treatment (Figures 7A-B). Importantly, the highest level of $p27^{KIP1}$ degradation activity was observed in the intact VP, while castration abolished this activity almost completely.

Some degradation of $p21^{WAF1}$, which is also a target of the ubiquitin-proteasome pathway (60-63), was noted in all the samples tested (Figure 6B). However, in contrast to $p27^{KIP1}$, the levels of $p21^{WAF1}$ degradation activity remained stable (Figures 7A-B).

Expression of $p27^{KIP1}$ transcripts during the androgen-induced regeneration of castrated rat VP

We also investigated whether $p27^{KIP1}$ and $p21^{WAF1}$ mRNA levels were modulated in the regenerating VP of castrated rats using Taqman® Real-Time RT-PCR. After inducing a drop in the level of $p27^{KIP1}$ transcripts at 12 hours of treatment (2.6 fold decrease), sustained T administration resulted in a slight but consistent increase in $p27^{KIP1}$ mRNA levels, which peaked at 96 hours of treatment (2.3 fold induction) (Figure 7D). The highest level of $p27^{KIP1}$ transcripts was detected in the VP from intact rats. On the other hand, $p21^{WAF1}$ mRNA levels were gradually and substantially upregulated, with maximal levels attained at 96 hours of T treatment (5.7 fold induction). Also, the level of $p21^{WAF1}$ transcripts was almost 3 times higher in the VP of intact rats than that in the VP of untreated castrated animals. Thus, our results strongly suggest that testosterone regulates $p27^{KIP1}$ expression mainly through its ubiquitin-proteasome-mediated degradation while it transcriptionally induces $p21^{WAF1}$ expression in the regenerating rat prostate.

DISCUSSION

In the present study, we have used a castration-regeneration rat prostate model for investigating the *in vivo* regulation of $p27^{KIP1}$ expression by androgens. In agreement with other reports, our results demonstrate that sustained T administration to castrated rats stimulates VP epithelial cell proliferation, whose rate peaks at 72 hours of androgen replenishment and then declines despite further treatment (1, 3, 5, 64-66).

Using Western blot experiments, we show that the castration-induced atrophy of the VP is associated with a significant upregulation of $p27^{KIP1}$ expression as compared with the VP of intact animals. In addition, T administration to castrated rats induces an early (12 hours) and substantial drop in $p27^{KIP1}$ levels while the expression levels of several G1-associated cdks and cyclins remains unchanged. This significant decrease in $p27^{KIP1}$ expression levels is also detected by immunohistochemistry in both basal and secretory cells. Furthermore, the amount of $p27^{KIP1}$ bound to cdk2, its main target, declines markedly in the early phase of T replenishment, suggesting a release in the inhibition of cdk2 activity. Together, these results thus indicate that the initial downregulation of $p27^{KIP1}$ in the androgen-induced regeneration of castrated rats VP may represent a primary cell cycle event, thereby allowing VP epithelial cells to proliferate.

Unexpectedly, the level of $p27^{KIP1}$ expression detected by Western blot peaks at the same time as the rate of epithelial cell proliferation and the levels of G1-related cdks and cyclins are maximal. Findings from our immunohistochemical experiments have helped clarify this paradoxical observation. First, the levels of $p27^{KIP1}$ strictly parallel those detected by Western blot in the corresponding total protein extracts during the course of T treatment, indicating that the changes in $p27^{KIP1}$ expression detected in the crude homogenates are representative of those occurring in the VP epithelial compartment. Second, when the rate of cell proliferation reaches its maximum, the majority of epithelial cells express $p27^{KIP1}$ whereas a minority of them proliferate. Third, the

detection of BrdU and the expression of $p27^{KIP1}$ in epithelial cells are mutually exclusive. In addition, the increased levels of $p27^{KIP1}$ expression detected at peak T-induced proliferation are coincident with an increased association of $p27^{KIP1}$ with, and presumably inhibition of, cdk2. Since cells expressing $p27^{KIP1}$ are BrdU-negative, our results indicate that in this model, $p27^{KIP1}$ may play a significant role in controlling the regrowth and restoring the glandular structure of the VP by limiting the proliferation of epithelial cells and favoring their post-mitotic differentiation. Further evidence is provided by our observation that, concomitant with the androgen-stimulated enhancement of cell proliferation and progressive reconstitution of VP morphology, $p27^{KIP1}$ expression is significantly induced only in non-proliferating secretory cells. It is also noteworthy that, in the VP of intact rats, the percentage of $p27^{KIP1}$-positive cells is also significantly higher in the secretory compartment than in the basal one. This is in keeping with the wide expression of $p27^{KIP1}$ in human prostate secretory cells as compared with the more restricted expression of this protein in basal cells (67) and the lack of its expression in the putative, transiently proliferating intermediate cell compartment (52). Altogether, our results thus add weight to the body of data indicating an important role for $p27^{KIP1}$ in the switch from proliferation to differentiation of precursor/progenitor cells from different lineages (41-48, 68).

In the VP of untreated castrated rats, $p27^{KIP1}$ expression levels are significantly higher in basal than in secretory cells. We have observed a similar though more striking pattern of selective distribution of $p27^{KIP1}$ expression in the VP gland of rats that had been castrated for 4 months. In those rats, a high level of anti-$p27^{KIP1}$ nuclear reactivity is detected in virtually all basal cells while residual secretory cells are consistently devoid of any staining (Loda M., Leav I. & Waltregny D., unpublished data). Since basal cells do not suffer a substantial loss in number following castration (3), it is tempting to hypothesize that the sustained, high expression of $p27^{KIP1}$ observed in basal cells after castration may be related to the suggested role of this protein in the prevention of cell

death. Recent studies on $p27^{KIP1-/-}$ mice have revealed an anti-apoptotic role of $p27^{KIP1}$ in growth-factor deprived mesangial cells and fibroblasts (69). $p27^{KIP1}$ also protects cells from cycloheximide-induced apoptosis (69) and has been shown to inhibit apoptosis following inflammatory injuries in renal glomerular and tubular cells (70). In a human leukemia cell line, overexpression of $p27^{KIP1}$ confers resistance to induction of apoptosis by several cytotoxic agents (71). Thus, although our hypothesis that $p27^{KIP1}$ overexpression may safeguard basal cells from androgen deprivation-induced apoptosis remains at this time highly speculative, it certainly deserves further investigation.

It is known that $p27^{KIP1}$ expression can be regulated at multiple levels (49) but the relative contribution of transcriptional, translational, or proteolytic control to $p27^{KIP1}$ regulation in various physiologic and pathologic contexts in the prostate gland remains largely unknown. Our results provide the first *in vivo* demonstration that androgens regulate $p27^{KIP1}$ expression mainly through ubiquitin-proteasome-mediated degradation. In fact, the maximal level of $p27^{KIP1}$ degradation activity is observed in the VP of intact animals, whereas castration abrogates this activity almost completely. Progressive restoration of $p27^{KIP1}$ degradation activity is obtained with T replenishment. In contrast to the $p21^{WAF1}$ gene, to date, no androgen response element has been found in the cloned portion of the $p27^{KIP1}$ gene promoter (72). Our results reveal that T treatment slightly modulates $p27^{KIP1}$ transcription in the VP of castrated rats. However, in view of the kinetics and magnitude of changes in $p27^{KIP1}$ mRNA expression, androgen-mediated $p27^{KIP1}$ transcriptional regulation, alone, is insufficient to explain the levels of $p27^{KIP1}$ protein expression detected during the course of the treatment. Furthermore, since the highest level of $p27^{KIP1}$ transcripts is found in the VP of intact rats while the protein level is the lowest, we conclude that in the VP of sexually mature rats T induces a high $p27^{KIP1}$ protein turnover by augmenting its proteasome-mediated degradation.

The regulation of $p27^{KIP1}$ proteasome-mediated proteolytic activity in the regenerating prostate may be specific for this protein. Indeed, the levels of $p21^{WAF1}$ degradation activity, another

target of the ubiquitin-proteasome pathway (60-63), remain unchanged during the course of T treatment and thus can not account for the gradual increase in expression levels of this protein observed during T treatment. In fact, it has been shown that the $p21^{WAF1}$ gene can be transcriptionally activated by androgens *in vitro* through binding of AR with an androgen response element present in its proximal promoter (73). In this report, we substantiate these findings in an *in vivo* model by demonstrating that the levels of $p21^{WAF1}$ transcripts are significantly upregulated by androgens.

In summary, the results from the present study convincingly suggest that $p27^{KIP1}$ plays an important role in the control of testosterone-stimulated proliferation and differentiation of normal prostate epithelial cells and that the regulation of $p27^{KIP1}$ levels by testosterone in those cells is achieved through modulation of its specific degradation by the ubiquitin-proteasome proteolytic system. We are currently conducting further investigations to elucidate how androgens are able to regulate $p27^{KIP1}$ proteasome-mediated degradation.

FIGURE LEGENDS

Figure 1. Epithelial cell proliferation in the ventral prostate of castrated rats treated by testosterone.

A. Castrated rats were treated by testosterone (T, 6.6mg/kg, once daily) for 4 days. At 0, 12, 24, 48, and 96 hours after the initiation of the treatment, rats (seven per time point) were injected with BrdU (10 mM) and sacrificed 30 minutes later. Seven untreated non-castrated age-matched male rats were also included as control animals. Tissue sections were cut from each paraffin-embedded VP sample, immunostained with an anti-BrdU monoclonal antibody, and counterstained with hematoxylin as described in *Materials and Methods*. Representative examples of BrdU immunodetection are shown for each group of 7 rats. Positive staining was completely abolished when the primary antibody was omitted from the staining procedure (data not shown). Original magnification: x200. *Inset,* detection of anti-BrdU immunoreactivity in the nucleus of both secretory and basal cells. *Arrow,* identification of a BrdU-positive epithelial cell.

B. Epithelial cell proliferation rates in the VP of castrated rats treated by T. The percentage of proliferating epithelial cells in the VP of each animal was calculated by dividing the number of BrdU-positive epithelial cells by the total number of epithelial cells counted (≈1000 cells). Assessment of the percentage of BrdU-positive epithelial cells was also done in the VP of 7 intact rats. Values are expressed as the mean ± standard error (*error bar*) for each group of 7 animals.

Figure 2. Expression of G1 phase-related cyclin-dependent kinases, cyclins and cyclin-dependent kinase inhibitors in the ventral prostate of testosterone-treated castrated rats.

Castrated rats (7 per time point) were sacrificed 0, 12, 24, 48, 72 and 96 hours after the beginning of androgen replenishment (6.6 mg/kg testosterone, once daily). The ventral prostate (VP) of each animal was harvested. VP specimens from 7 age-matched intact animals were also used. Tissue

sample duplicates for each group of 7 rats were obtained by pooling separately the VP specimens from 3 and 4 animals. Total proteins were extracted from the pooled samples. Protein lysates (100 μg per sample) were subjected to Western blot analysis of androgen receptor (AR), cdk2, cdk4, cdk6, cyclin D1, cyclin E, $p21^{WAF1}$ and $p27^{KIP1}$ expression, as described in *Materials and Methods*. Ponceau S staining of the membranes showed equal protein sample loading and transferring (data not shown). Each Western blot experiment was performed at least twice with both sets of pooled samples and consistent results were observed. Fold increases (+) or decreases (-) in $p27^{KIP1}$ protein levels quantified by ImageQuant™ program are indicated under the Western blot.

Figure 3. *In situ* expression of $p27^{KIP1}$ in the regenerating ventral prostate of castrated rats.

A. Immunodetection of $p27^{KIP1}$ in the ventral prostate (VP) of castrated rats treated by testosterone (T). Following treatment by T (6.6 mg/kg, once daily) for the indicated times, castrated rats (7 per time point) were sacrificed and the VP from each animal was harvested. Seven intact age-matched male rats were also used. Tissue sections from each paraffin-embedded VP were cut, immunostained with an anti-$p27^{KIP1}$ monoclonal antibody, and counterstained with hematoxylin as described in *Materials and Methods*. Representative examples of $p27^{KIP1}$ staining are shown for each group of 7 animals. Substitution of the primary antibody with PBS did not yield any specific staining (data not shown). Original magnification: x400.

B. Levels of $p27^{KIP1}$ expression in the VP of castrated rats treated by T, as determined by immunohistochemistry. Scoring of $p27^{KIP1}$ immunostaining in the VP of each rat was done according to the percentage of epithelial cells (≈500 cells counted) exhibiting nuclear anti-$p27^{KIP1}$ reactivity. $p27^{KIP1}$ scoring was also done in the VP of 7 intact rats. $p27^{KIP1}$ scores were determined in the basal *(open diamonds)* and secretory *(closed circles)* cell subsets separately. All scoring values are expressed as the mean ± standard error *(error bar)* for each group of 7 rats. The paired t-

test was used to assess whether there were significant differences in $p27^{KIP1}$ expression levels between basal and secretory cells at each treatment time point. Statistically significant differences are indicated as asterisks (*: $P< 0.05$; **: $P< 0.01$; ***: $P< 0.005$).

Figure 4. Absence of $p27^{KIP1}$ expression in proliferating epithelial cells from the regenerating ventral prostate of castrated rats.

Double immunofluorescence staining for $p27^{KIP1}$ and BrdU was performed in paraffin-embedded VP specimens from 7 castrated rats that had been sacrificed after 3 days of continuous testosterone treatment (6.6 mg/kg, once daily). Tissue sections from each VP were immunostained with an anti-$p27^{KIP1}$ antibody and detection was performed utilizing fluorescein isothiocyanate (FITC)-conjugated (see *Materials and Methods*). Subsequently, the same sections were immunostained with anti-BrdU monoclonal antibody and detection was done using Texas Red-conjugated streptavidin (see *Materials and Methods*). Substitution of the primary antibodies with PBS did not yield any specific staining. Photomicrographs of double immunofluorescence staining for $p27^{KIP1}$ and BrdU in a representative prostate gland were taken under an UV microscope using appropriate filters for detecting FITC/$p27^{KIP1}$ (A), Texas Red/BrdU (B), and both FITC/$p27^{KIP1}$ and Texas Red/BrdU (C).

Figure 5. Association of $p27^{KIP1}$ with cdk2 in the regenerating prostate of castrated rats.

Following treatment by testosterone (T, 6.6 mg/kg, once daily) for the indicated times, castrated rats (7 per time point) were sacrificed and the VP from each animal was harvested. The VP from 7 intact age-matched male rats was also collected. The VP specimens from each group of 7 rats were randomly pooled in duplicates containing 3 and 4 VP specimens, each. Total proteins were extracted and used in cdk2/$p27^{KIP1}$ co-immunoprecipitation experiments. A. Protein lysates (500μg

per sample) were immunoprecipitated with 1.5 μg of anti-cdk2 antibody, as detailed in *Materials and Methods*. The immunoprecipitates were subjected to SDS-PAGE and transferred to nitrocellulose membranes, which were blotted with an anti-$p27^{KIP1}$ antibody. Immunoprecipitates of VP lysates (500μg) from rats treated by T for 72 hours with 1.5 μg of rabbit immunoglobulins G (IgG) were used as negative controls. 100 μg of non-immunoprecipitated intact VP protein lysates were also used in the Western blotting procedure. Co-immunoprecipitation experiments were performed with both sets of pooled samples and yielded reproducible results. B. $p27^{KIP1}$-probed membranes were subsequently stripped and reprobed with an anti-cdk2 antibody to examine the amount of cdk2 in the different samples.

Figure 6. Kinetics of $p27^{KIP1}$ and $p21^{WAF1}$ degradation in the regenerating ventral prostate of castrated rats.

Following treatment by testosterone (6.6 mg/kg, im, once daily) for the indicated times, castrated rats (7 per time point) were sacrificed the VP from each animal was harvested. The VP from 7 intact age-matched male rats was also collected. The VP specimens from each group of 7 rats were randomly pooled in duplicates containing 3 and 4 VP specimens, each. Total proteins were isolated from each pooled sample. Purified human recombinant his_6-tagged $p27^{KIP1}$ (A) and $p21^{WAF1}$ (B) proteins (300 ng) were incubated for the indicated times at 37°C in the presence of a degradation mix containing 100 μg of each VP protein lysate, as described in *Materials and Methods*. The degradation of the his_6-tagged proteins by the lysates was analyzed by immunoblotting with an anti-histidine antibody. Each degradation assay was performed at least twice with both sets of pooled samples and consistent results were observed. Control experiments included the omission of the lysates from the degradation mix. No specific signal was obtained when the tagged proteins were not added to the degradation mix (data not shown). C. Protein lysates (100 μg) from the VP of intact

animals were assayed for his_6-$p27^{KIP1}$ degradation activity in presence or absence of the proteasome inhibitor MG-132 (100 μM) in the degradation mixture.

Figure 7. Androgen regulation of $p27^{KIP1}$ and $p21^{WAF1}$ expression in the regenerating prostate of castrated rats.

Following treatment by testosterone (T) for the indicated times, castrated rats (7 per time point) were sacrificed and the VP from each animal was harvested. The VP from 7 intact age-matched male rats was also harvested. The VP specimens from each group of 7 rats were randomly pooled in duplicates containing 3 and 4 VP specimens, each. A. Purified human recombinant his_6-tagged $p27^{KIP1}$ and $p21^{WAF1}$ proteins (300 ng) were incubated for 0 hour and 4 hours at 37°C in the presence of a degradation mix containing 100 μg of VP protein lysate, as described in *Materials and Methods*. The degradation activity of the lysates for the his_6-tagged proteins was analyzed by immunoblotting with an anti-histidine antibody. Each degradation assay was performed at least twice with both sets of pooled samples and consistent results were observed. B. Quantification of degradation activity for the exogenous proteins was done by densitometric analysis of the bands at ±22kDa and ±28kDa corresponding to undegraded his_6-tagged $p21^{WAF1}$ and $p27^{KIP1}$ proteins, respectively. Relative degradation activity of the samples at each time point following T injections (*closed circles*) was calculated by dividing the densitometric volume of the band obtained with the sample without incubation (0 hour) by the one obtained with the sample incubated for 4 hours in the degradation mix. Relative levels of $p27^{KIP1}$ and $p21^{WAF1}$ degradation activity were correlated with the endogenous levels of these proteins (*open diamonds*) in the VP at each time point (see Figure 2). All values are normalized to those found in the VP of untreated castrated rats. C. Total RNA was extracted from each VP tissue duplicate. 1 μg of total RNA per sample was reverse-transcribed and a twentieth of each RT reaction was subjected to Taqman® Real-Time PCR amplification, as

described in *Materials and Methods*. The specific rat $p27^{KIP1}$ and $p21^{WAF1}$ primers and probes used in the PCR reactions are shown in Table 1. The housekeeping GAPDH gene was used as endogenous control. The relative amounts of $p27^{KIP1}$ and $p21^{WAF1}$ transcripts in each sample were determined using the standard curve method and were normalized to GAPDH mRNA expression levels. All values represent the mean of triplicates and are normalized to those found in the VP of untreated castrated rats. Error bars stand for standard deviations. Taqman® PCR experiments were performed with both sets of pooled samples and consistent results were observed. PCR reactions with samples in which the Reverse Transcriptase or the target RNA was omitted from the reverse transcription reaction did not yield any significant amplification (data not shown).

ACKNOWLEDGMENTS

The authors thank Jane Hayward for help in preparing the manuscript, and William Sellers and Miles Brown for critical comments on this manuscript.

This work was supported by DOD grant # PC970273.

REFERENCES

1. Cunha GR, Donjacour AA, Cooke PS, Mee S, Bigsby RM, Higgins SJ, Sugimura Y 1987 The endocrinology and developmental biology of the prostate. Endocr Rev 8:338-362.
2. Evans GS, Chandler JA 1987 Cell proliferation studies in the rat prostate: I. The proliferative role of basal and secretory cells during normal growth. Prostate 10:163-178.
3. English HF, Santen RJ, Isaacs JT 1987 Response of glandular versus basal rat ventral prostatic epithelial cells to androgen withdrawal and replacement. Prostate 11:229-242.
4. Isaacs JT, Lundmo PI, Berges R, Martikainen P, Kyprianou N, English HF 1992 Androgen regulation of programmed death of normal and malignant prostatic cells. J Androl 13:457-464.
5. Bruchovsky N, Lesser B, Van Dorne E, Craven S 1975 Hormonal effects on cell proliferation in rat prostate. Vitam Horm 33:61-102.
6. Ho SM, Damassa D, Kwan PW, Seto HS, Leav I 1985 Androgen receptor levels and androgen contents in the prostate lobes of intact and testosterone-treated Noble rats. J Androl 6:279-290.
7. Chen Y, Robles AI, Martinez LA, Liu F, Gimenez-Conti IB, Conti CJ 1996 Expression of G1 cyclins, cyclin-dependent kinases, and cyclin-dependent kinase inhibitors in androgen-induced prostate proliferation in castrated rats. Cell Growth Differ 7:1571-1578.
8. Leav I, Merk FB, Kwan PW, Ho SM 1989 Androgen-supported estrogen-enhanced epithelial proliferation in the prostates of intact Noble rats. Prostate 15:23-40.
9. Wang X, Hsieh JT 1994 Androgen repression of cytokeratin gene expression during rat prostate differentiation: evidence for an epithelial stem cell-associated marker. Chin Med Sci J 9:237-241.
10. English HF, Drago JR, Santen RJ 1985 Cellular response to androgen depletion and repletion in the rat ventral prostate: autoradiography and morphometric analysis. Prostate 7:41-51.
11. Katz AE, Benson MC, Wise GJ, Olsson CA, Bandyk MG, Sawczuk IS, Tomashefsky P, Buttyan R 1989 Gene activity during the early phase of androgen-stimulated rat prostate regrowth. Cancer Res 49:5889-5894.
12. Epner DE, Partin AW, Schalken JA, Isaacs JT, Coffey DS 1993 Association of glyceraldehyde-3-phosphate dehydrogenase expression with cell motility and metastatic potential of rat prostatic adenocarcinoma. Cancer Res 53:1995-1997.
13. Morgan DO 1997 Cyclin-dependent kinases: engines, clocks, and microprocessors. Annu Rev Dev Biol 13:261-291.
14. Sherr CJ 1996 Cancer cell cycles. Science 274:1672-1677.
15. Elledge SJ 1996 Cell cycle checkpoints: preventing an identity crisis. Science 274:1664-1671.
16. DelSal G, Loda M, Pagano M 1996 Cell cycle and cancer: critical events at the G1 restriction point. Crit Rev Oncog 7:127-142.
17. Sherr CJ, Roberts JM 1999 CDK inhibitors: positive and negative regulators of G1-phase progression. Genes Dev 13:1501-1512.
18. Hengst L, Reed SI 1998 Inhibitors of the Cip/Kip family. Curr Top Microbiol Immunol 227:25-41.

19. Polyak K, Kato JY, Solomon MJ, Sherr CJ, Massague J, Roberts JM, Koff A 1994 p27Kip1, a cyclin-Cdk inhibitor, links transforming growth factor-beta and contact inhibition to cell cycle arrest. Genes Dev 8:9-22.

20. Polyak K, Lee M-H, Erdjument-Bromage A, Koff A, Roberts JM, Tempst P, Massague J 1994 Cloning of p27KIP1, a cyclin-dependent kinase inhibitor and a potential mediator of extracellular antimitogenic signals. Cell 78:59-66.

21. Toyoshima H, Hunter T 1994 p27, a novel inhibitor of G1 cyclin-Cdk protein kinase activity, is related to p21. Cell 78:67-74.

22. Fang F, Orend G, Watanabe N, Hunter T, Ruoslahti E 1996 Dependence of cyclin E-CDK2 kinase activity on cell anchorage. Science 271:499-502.

23. Kato J, Matsuoka M, Polyak K, Massague J, Sherr CJ 1994 Cyclic AMP-induced G1 phase arrest mediated by an inhibitor (p27KIP1) of cyclin-dependent kinase 4 activation. Cell 79:487-496.

24. Kuniyasu H, Yasui W, Kitahara K, Naka K, Yokozaki H, Akama Y, Hamamoto T, Tahara H, Tahara E 1997 Growth inhibitory effect of interferon-ß is associated with the induction of cyclin-dependent kinase inhibitor p27KIP1 in a human gastric carcinoma cell line. Cell Growth Differ 8:47-52.

25. Harvat BL, Seth P, Jetten AM 1997 The role of p27KIP1 in gamma-interferon-mediated growth arrest of mammary epithelial cells and related defects in mammary carcinoma cells. Oncogene 14:2111-2122.

26. Kortylewski M, Heinrich PC, Mackiewicz A, Schniertshauer U, Klingmuller U, Nakajima K, Hirano T, Horn F, Behrmann I 1999 Interleukin-6 and oncostatin M-induced growth inhibition of human A375 melanoma cells is STAT-dependent and involves upregulation of the cyclin-dependent kinase inhibitor p27/KIP1. Oncogene 18:3742-3753.

27. Nourse J, Firpo E, Flanagan WM, Coats S, Polyak K, Lee MH, Massague J, Crabtree GR, Roberts JM 1994 Interleukin-2-mediated elimination of the p27Kip1 cyclin-dependent kinase inhibitor prevented by rapamycin. Nature 372:570-573.

28. Coats S, Flanagan WM, Nourse J, Roberts JM 1996 Requirement of p27Kip1 for restriction point control of the fibroblast cell cycle. Science 272:877-880.

29. Rivard N, L'Alleimain G, Bartek J, Pouyssegur J 1996 Abrogation of p27KIP1 by cDNA antisense suppresses quiescence (G0 state) in fibroblasts. J Biol Chem 271:18337-18341.

30. Sheaff RJ, Groudine M, Gordon M, Roberts JM, Clurman BE 1997 Cyclin E-CDK2 is a regulator of p27Kip1. Genes Dev 11:1464-1478.

31. Montagnoli A, Fiore F, Eytan E, Carrano AC, Draetta GF, Hershko A, Pagano M 1999 Ubiquitination of p27 is regulated by Cdk-dependent phosphorylation and trimeric complex formation. Genes Dev 13:1181-1189.

32. Nguyen H, Gitig DM, Koff A 1999 Cell-free degradation of p27(kip1), a G1 cyclin-dependent kinase inhibitor, is dependent on CDK2 activity and the proteasome. Mol Cell Biol 19:1190-1201.

33. Vlach J, Hennecke S, Amati B 1997 Phosphorylation-dependent degradation of the cyclin-dependent kinase inhibitor p27. EMBO J 16:5334-5344.

34. Carrano AC, Eytan E, Hershko A, Pagano M 1999 SKP2 is required for ubiquitin-mediated degradation of the CDK inhibitor p27. Nat Cell Biol 1:193-199.

35. Tsvetkov LM, Yeh KH, Lee SJ, Sun H, Zhang H 1999 p27(Kip1) ubiquitination and degradation is regulated by the SCF(Skp2) complex through phosphorylated Thr187 in p27. Curr Biol 9:661-664.

36. Pagano M, Tam SW, Theodoras AM, Beer-Romero P, Del Sal G, Chau V, Yew PR, Draetta GF, Rolfe M 1995 Role of the ubiquitin-proteasome pathway in regulating abundance of the cyclin-dependent kinase inhibitor p27. Science 269:682-685.

37. Medema RH, Kops GJ, Bos JL, Burgering BM 2000 AFX-like Forkhead transcription factors mediate cell-cycle regulation by Ras and PKB through p27kip1. Nature 404:782-787.

38. Menjo M, Kaneko Y, Ogata E, Ikeda K, Nakanishi M 1998 Critical role for p27Kip1 in cell cycle arrest after androgen depletion in mouse mammary carcinoma cells (SC-3). Oncogene 17:2619-2627.

39. Cordon-Cardo C, Koff A, Drobnjak M, Capodieci P, Osman I, Millard SS, Gaudin PB, Fazzari M, Zhang ZF, Massague J, Scher HI 1998 Distinct altered patterns of p27KIP1 gene expression in benign prostatic hyperplasia and prostatic carcinoma. J Natl Cancer Inst 90:1284-1291.

40. Millard SS, Yan JS, Nguyen H, Pagano M, Kiyokawa H, Koff A 1997 Enhanced ribosomal association of p27(Kip1) mRNA is a mechanism contributing to accumulation during growth arrest. J Biol Chem 272:7093-7098.

41. Hengst L, Reed SI 1996 Translational control of p27Kip1 accumulation during the cell cycle. Science 271:1861-1864.

42. Fero ML, Rivkin M, Tasch M, Porter P, Carow CE, Firpo E, Polyak K, Tsai LH, Broudy V, Perlmutter RM, Kaushansky K, Roberts JM 1996 A syndrome of multiorgan hyperplasia with features of gigantism, tumorigenesis, and female sterility in p27(Kip1)-deficient mice. Cell 85:733-744.

43. Kiyokawa H, Kineman RD, Manova-Todorova KO, Soares VC, Hoffman ES, Ono M, Khanam D, Hayday AC, Frohman LA, Koff A 1996 Enhanced growth of mice lacking the cyclin-dependent kinase inhibitor function of p27(Kip1). Cell 85:721-732.

44. Nakayama K, Ishida N, Shirane M, Inomata A, Inoue T, Shishido N, Horii I, Loh DY 1996 Mice lacking p27(Kip1) display increased body size, multiple organ hyperplasia, retinal dysplasia, and pituitary tumors. Cell 85:707-720.

45. Tong W, Kiyokawa H, Soots TJ, Park MS, Soares VC, Manova K, Pollard JW, Koff A 1998 The absence of p27KIP1, an inhibitor of G1 cyclin-dependent kinases, uncouples differentiation and growth arrest during the granulosa-luteal transition. Cell Growth Differ 9:787-794.

46. Robker RL, Richards JS 1998 Hormone-induced proliferation and differentiation of granulosa cells: a coordinated balance of the cell cycle regulators cyclin D2 and p27Kip1. Mol Endocrinol 12:924-940.

47. Casaccia-Bonnefil P, Tikoo R, Kiyokawa H, Friedrich V, Chao MV, Koff A 1997 Oligodendrocyte precursor differentiation is perturbed in the absence of the cyclin-dependent kinase inhibitor p27KIP1. Genes Dev 11:2335-2346.

48. Drissi H, Hushka D, Aslam F, Nguyen Q, Buffone E, Koff A, van Wijnen A, Lian JB, Stein JL, Stein GS 1999 The cell cycle regulator p27kip1 contributes to growth and differentiation of osteoblasts. Cancer Res 59:3705-3711.

49. Sgambato A, Cittadini A, Faraglia B, Weinstein IB 2000 Multiple functions of p27(Kip1) and its alterations in tumor cells: a review. J Cell Physiol 183:18-27.

50. Mori S, Murakami-Mori K, Bonavida B 1999 Interleukin-6 induces G1 arrest through induction of p27(Kip1), a cyclin-dependent kinase inhibitor, and neuron-like morphology in LNCaP prostate tumor cells. Biochem Biophys Res Commun 257:609-614.

51. Zi X, Agarwal R 1999 Silibinin decreases prostate-specific antigen with cell growth inhibition via G1 arrest, leading to differentiation of prostate carcinoma cells: implications for prostate cancer intervention. Proc Natl Acad Sci U S A 96:7490-7495.

52. De Marzo AM, Meeker AK, Epstein JI, Coffey DS 1998 Prostate stem cell compartments: expression of the cell cycle inhibitor p27KIP1 in normal, hyperplastic, and neoplastic cells. Am J Pathol 153:911-919.

53. Tsihlias J, Zhang W, Bhattacharya N, Flanagan M, Klotz L, Slingerland J 2000 Involvement of p27Kip1 in G1 arrest by high dose 5 alpha-dihydrotestosterone in LNCaP human prostate cancer cells. Oncogene 19:670-679.

54. Kokontis JM, Hay N, Liao S 1998 Progression of LNCaP prostate tumor cells during androgen deprivation: hormone-independent growth, repression of proliferation by androgen, and role for p27Kip1 in androgen-induced cell cycle arrest. Mol Endocrinol 12:941-953.

55. Agus DB, Cordon-Cardo C, Fox W, Drobnjak M, Koff A, Golde DW, Scher HI 1999 Prostate cancer cell cycle regulators: response to androgen withdrawal and development of androgen independence. J Natl Cancer Inst 91:1869-1876.

56. Loda M, Cukor B, Tam SW, Lavin P, Fiorentino M, Draetta GF, Jessup JM, Pagano M 1997 Increased proteasome-dependent degradation of the cyclin-dependent kinase inhibitor p27 in aggressive colorectal carcinomas. Nat Med 3:231-234.

57. Chiarle R, Budel LM, Skolnik J, Frizzera G, Chilosi M, Corato A, Pizzolo G, Magidson J, Montagnoli A, Pagano M, Maes B, De Wolf-Peeters C, Inghirami G 2000 Increased proteasome degradation of cyclin-dependent kinase inhibitor p27 is associated with a decreased overall survival in mantle cell lymphoma. Blood 95:619-626.

58. Fink L, Seeger W, Ermert L, Hanze J, Stahl U, Grimminger F, Kummer W, Bohle RM 1998 Real-time quantitative RT-PCR after laser-assisted cell picking. Nat Med 4:1329-1333.

59. Thomas GV, Szigeti K, Murphy M, Draetta G, Pagano M, Loda M 1998 Down-regulation of p27 is associated with development of colorectal adenocarcinoma metastases. Am J Pathol 153:681-687.

60. Maki CG, Howley PM 1997 Ubiquitination of p53 and p21 is differentially affected by ionizing and UV radiation. Mol Cell Biol 17:355-363.

61. Maki CG, Huibregtse JM, Howley PM 1996 In vivo ubiquitination and proteasome-mediated degradation of p53. Cancer Res 56:2649-2654.

62. Yu ZK, Gervais JL, Zhang H 1998 Human CUL-1 associates with the SKP1/SKP2 complex and regulates p21(CIP1/WAF1) and cyclin D proteins. Proc Natl Acad Sci U S A 95:11324-11329.

63. Blagosklonny MV, Wu GS, Omura S, el-Deiry WS 1996 Proteosome-dependent regulation of p21WAF1/CIP1 expression. Biochem Biophys Res Commun 227:564-569.

64. Chung LWK, Coffey DS 1971 Biochemical characterization of prostatic nuclei. II. Relationship between DNA synthesis and protein synthesis. Biochim Biophys Acta 247:584.

65. Furuya Y, Lin XS, Walsh JC, Nelson WG, Isaacs JT 1995 Androgen ablation-induced programmed death of prostatic glandular cells does not involve recruitment into a defective cell cycle or p53 induction. Endo 136:1898-1906.

66. Evans GS, Chandler JA 1987 Cell proliferation studies in the rat prostate: II. The effects of castration and androgen-induced regeneration upon basal and secretory cell proliferation. Prostate 11:339-352.

67. Guo Y, Sklar GN, Borkowski A, Kyprianou N 1997 Loss of the cyclin-dependent kinase inhibitor p27(kip1) protein in human prostate cancer correlates with tumor grade. Clin Cancer Res 3:2269-2274.

68. Durand B, Gao FB, Raff M 1997 Accumulation of the p27/KIP1 cyclin-dependent kinase inhibitor and the timing of oligodendrocyte differentiation. EMBO J 16:306-317.

69. Hiromura K, Fero ML, Roberts JM, Shankland SJ 1999 Modulation of apoptosis by the cyclin-dependent kinase inhibitor p27KIP1. J Clin Invest 103:597-604.

70. Ophascharoensuk V, Fero ML, Hughes J, Roberts JM, Shankland SJ 1998 The cyclin dependent kinase inhibitor p27KIP1 safeguards against inflammatory injury. Nat Med 4:575-580.

71. Eymin B, Haugg M, Droin N, Sordet O, Dimanche-Boitrel M-T, Solary E 1999 p27KIP1 induces drug resistance by preventing apoptosis upstream of cytochrome c release and procaspase-3 activation in leukemic cells. Oncogene 18:1411-1418.

72. Minami S, Ohtani-Fujita N, Igata E, Tamaki T, Sakai T 1997 Molecular cloning and characterization of the human p27KIP1 gene promoter. FEBS Lett 411:1-6.

73. Lu S, Liu M, Epner DE, Tsai SY, Tsai MJ 1999 Androgen regulation of the cyclin-dependent kinase inhibitor p21 gene through an androgen response element in the proximal promoter. Mol Endocrinol 13:376-384.

Table 1. Sequences of primers and probes used for Taqman® PCR experiments.

Oligonucleotide name	Sequence
$p27^{KIP1}$ amplicon size: 128 bp	
$p27^{KIP1}$ forward primer	CCACAGTGCCAGCATTCG
$p27^{KIP1}$ reverse primer	TGGGTTAGCGGAGCAGTGT
$p27^{KIP1}$ hybridization probe	AATCTTCTGCCGCAGGTCGCTTCC
$p21^{WAF1}$ amplicon size: 124 bp	
$p21^{WAF1}$ forward primer	AGCAGTTGAGCCGCGATT
$p21^{WAF1}$ reverse primer	CGAACACGCTCCCAGACG
$p21^{WAF1}$ hybridization probe	CTTTGACTTCGCCACTGAGACGCCA

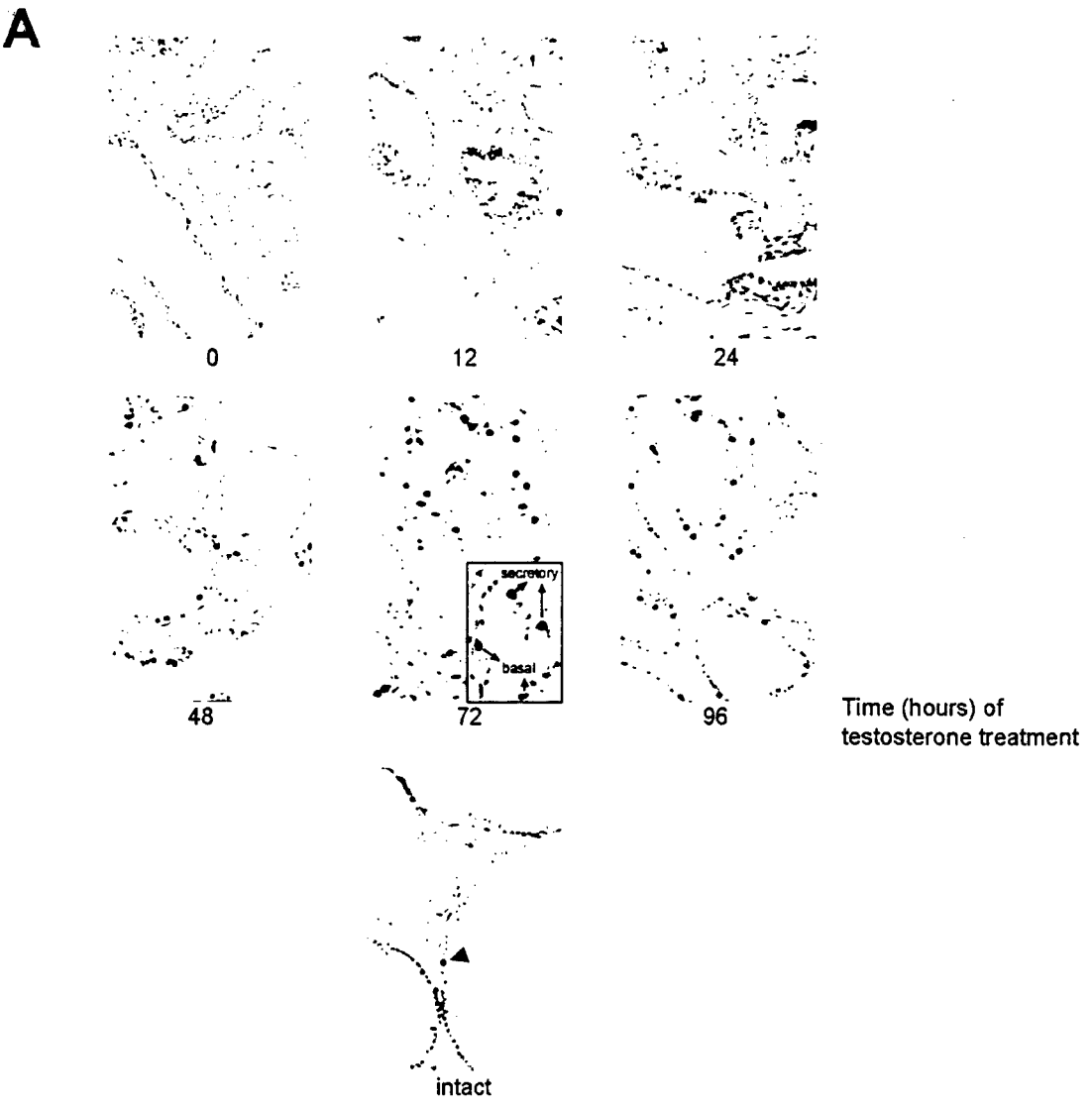
A
0
12
24
48
72
96
secretory
basal
Time (hours) of testosterone treatment
intact
B
BrdU-positive cells (%)
20
15
10
5
0
0
12
24
48
72
96
intact
Time (hours) of testosterone treatment

FIGURE 1

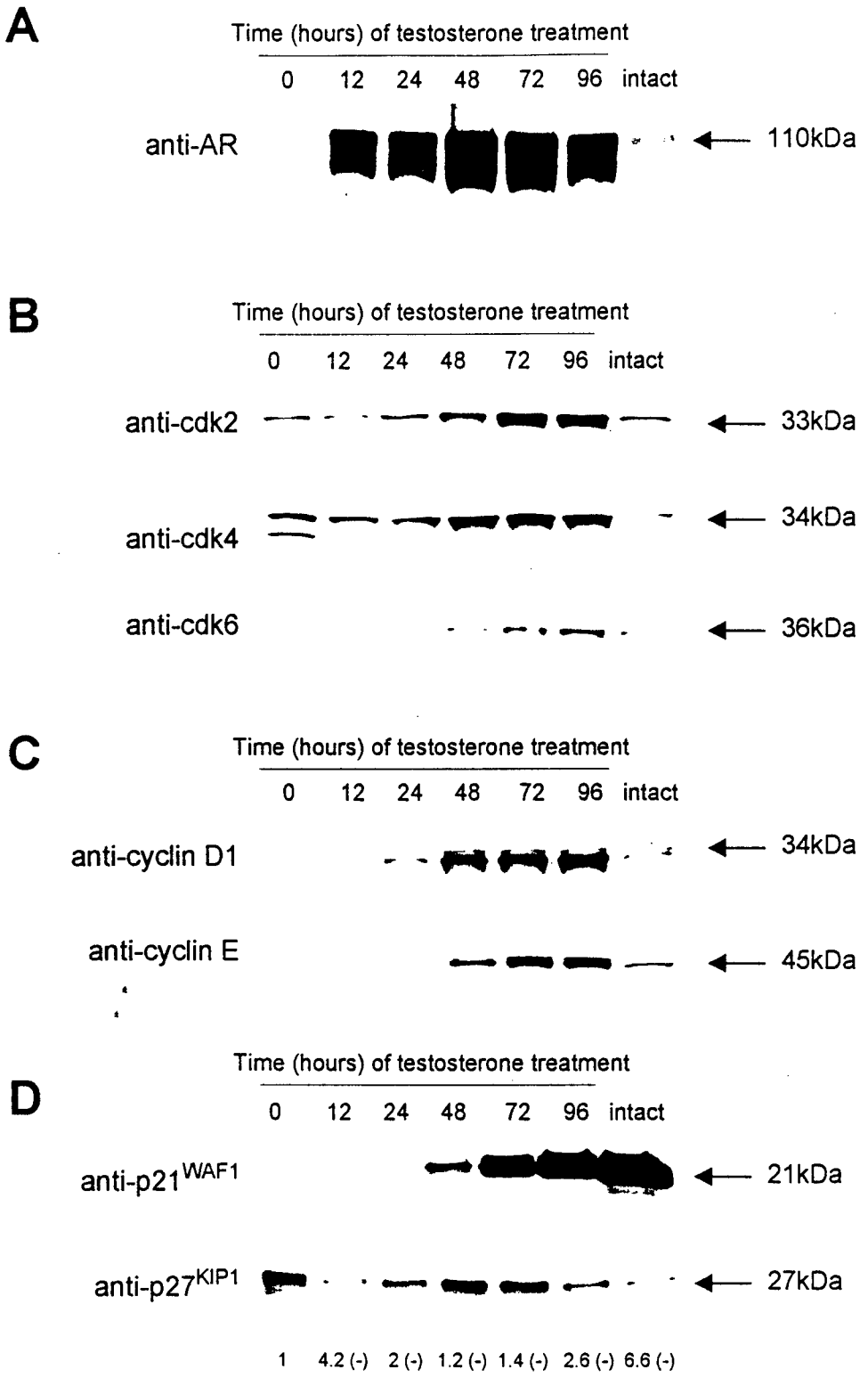
A
Time (hours) of testosterone treatment
0 12 24 48 72 96 intact
anti-AR
110kDa
B
Time (hours) of testosterone treatment
0 12 24 48 72 96 intact
anti-cdk2
33kDa
anti-cdk4
34kDa
anti-cdk6
36kDa
C
Time (hours) of testosterone treatment
0 12 24 48 72 96 intact
anti-cyclin D1
34kDa
anti-cyclin E
45kDa
D
Time (hours) of testosterone treatment
0 12 24 48 72 96 intact
anti-p21WAF1
21kDa
anti-p27KIP1
27kDa
1 4.2 (-) 2 (-) 1.2 (-) 1.4 (-) 2.6 (-) 6.6 (-)

FIGURE 2

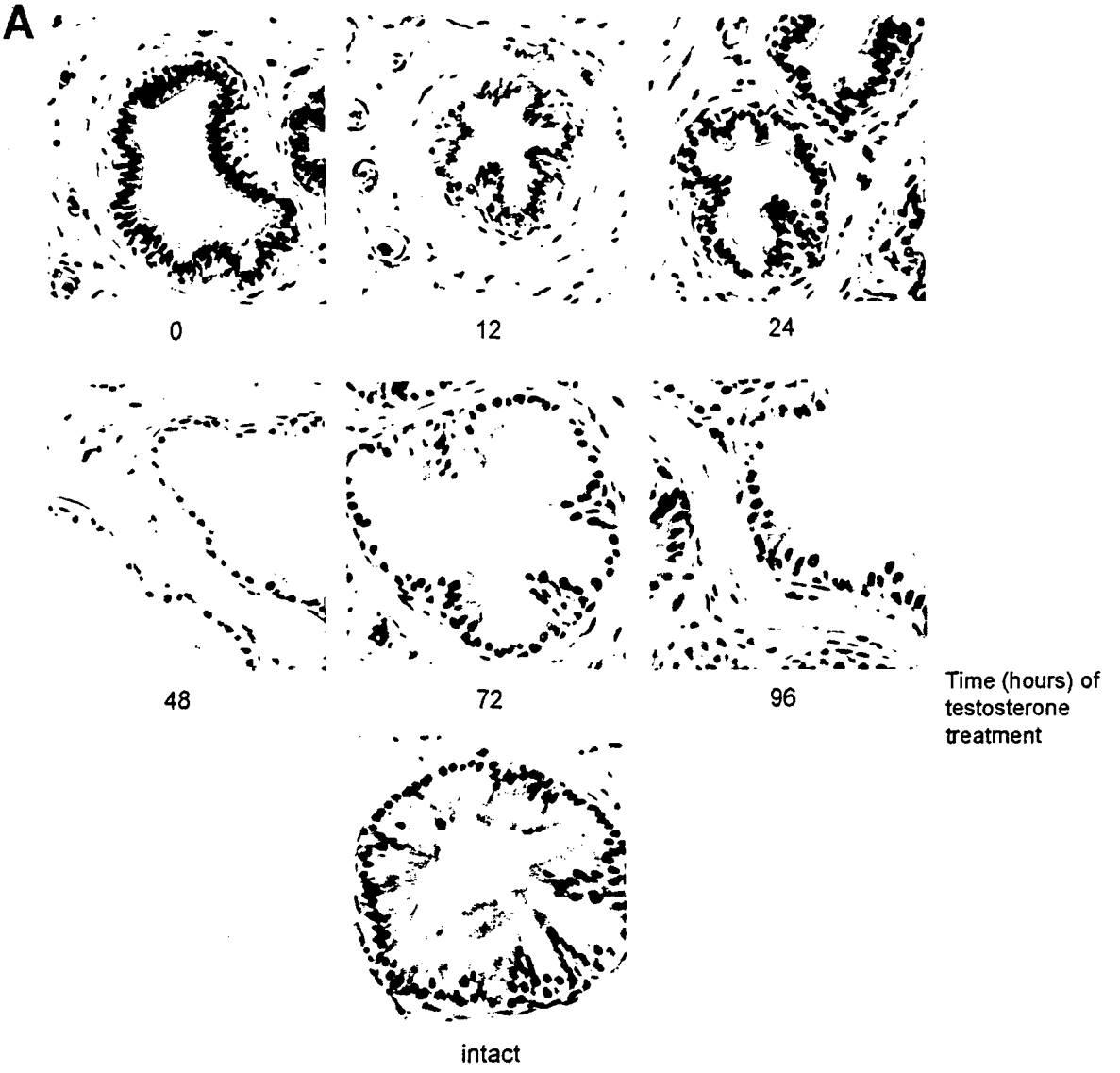
A
0
12
24
48
72
96
Time (hours) of testosterone treatment
intact
B
p27KIP1-positive cells (%)
100
80
60
40
20
0
0
12
24
48
72
96
intact
Time (hours) of testosterone treatment

FIGURE 3

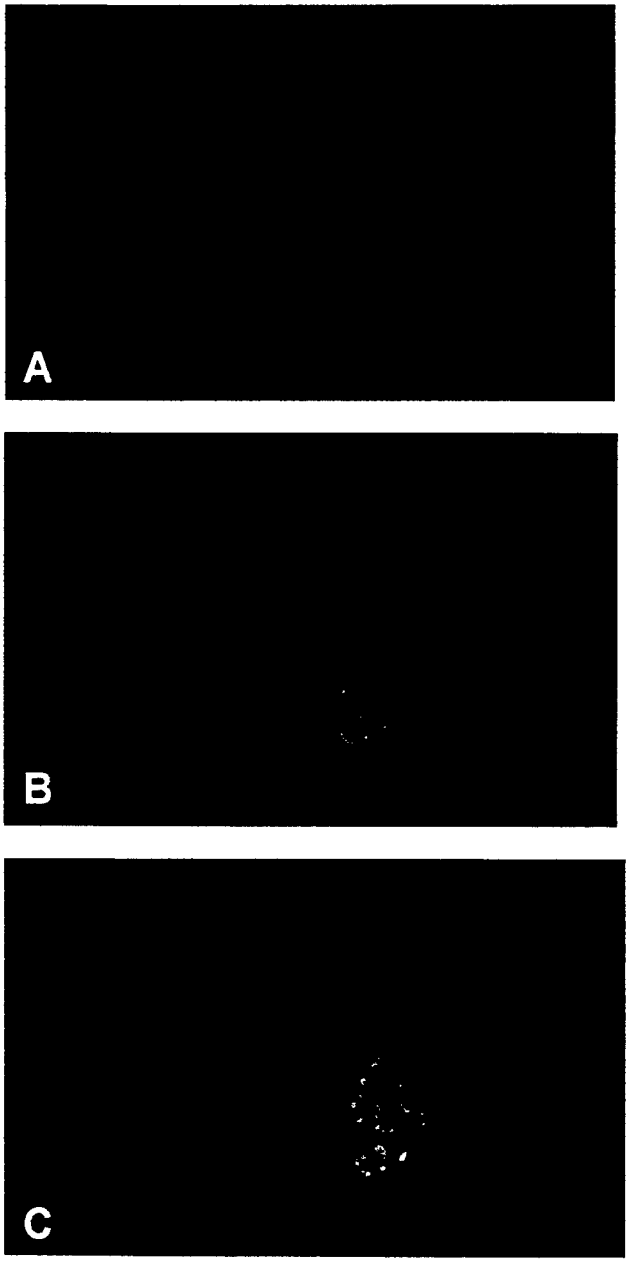

FIGURE 4

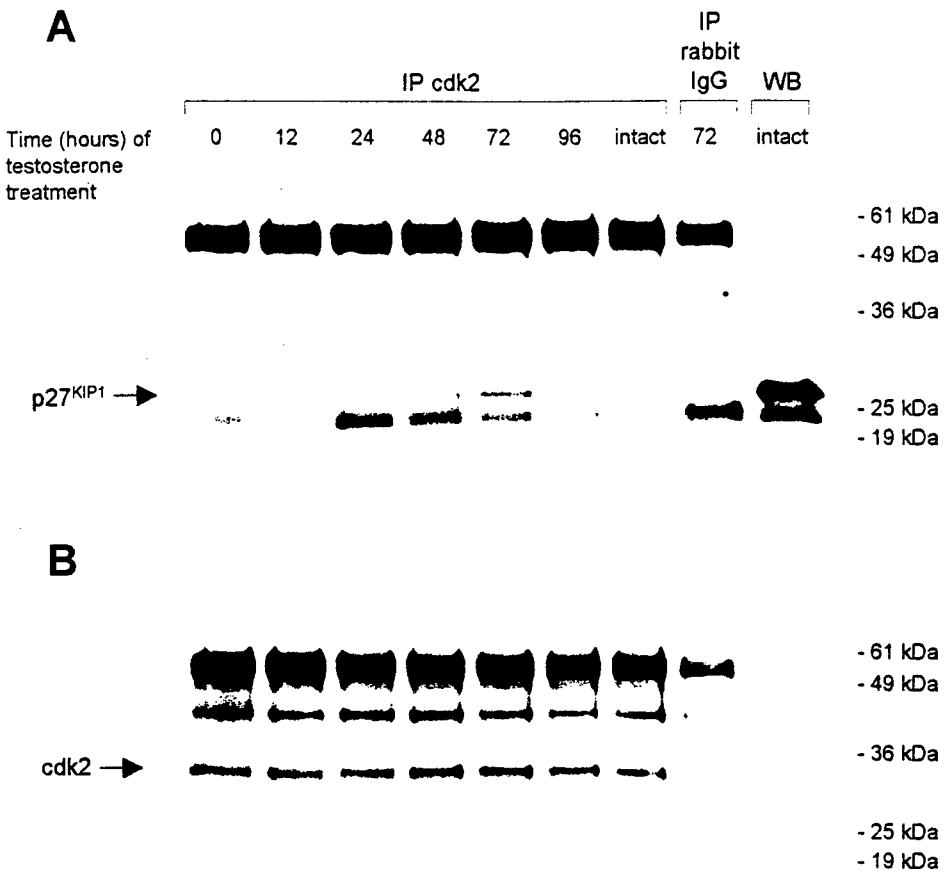
A
IP cdk2
IP rabbit IgG
WB
Time (hours) of testosterone treatment
0
12
24
48
72
96
intact
72
intact
- 61 kDa
- 49 kDa
- 36 kDa
p27KIP1
- 25 kDa
- 19 kDa
B
- 61 kDa
- 49 kDa
cdk2
- 36 kDa
- 25 kDa
- 19 kDa

FIGURE 5

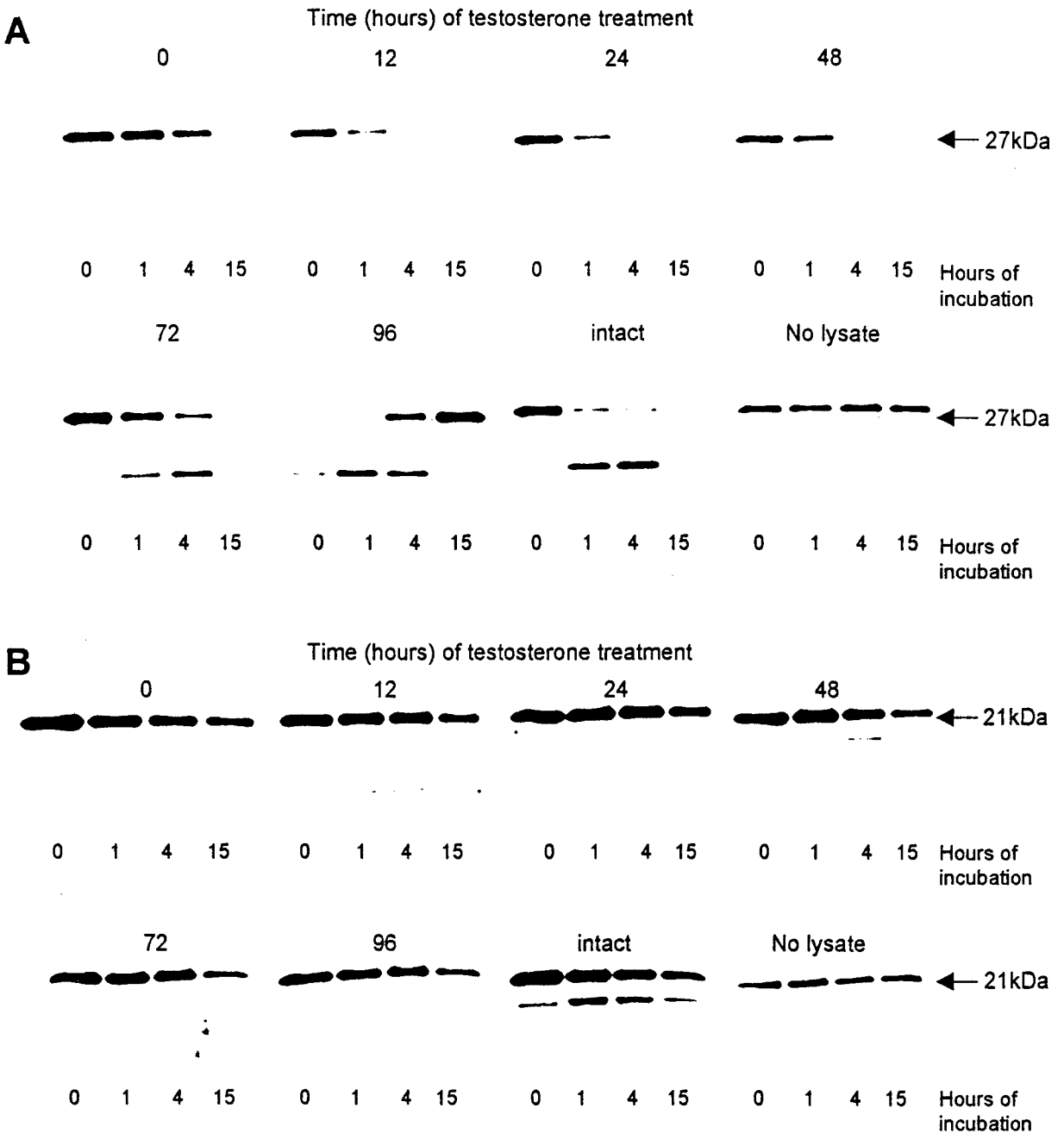
A
Time (hours) of testosterone treatment
0
12
24
48
27kDa
0 1 4 15 0 1 4 15 0 1 4 15 0 1 4 15
Hours of incubation
72
96
intact
No lysate
27kDa
0 1 4 15 0 1 4 15 0 1 4 15 0 1 4 15
Hours of incubation
B
Time (hours) of testosterone treatment
0
12
24
48
21kDa
0 1 4 15 0 1 4 15 0 1 4 15 0 1 4 15
Hours of incubation
72
96
intact
No lysate
21kDa
0 1 4 15 0 1 4 15 0 1 4 15 0 1 4 15
Hours of incubation
C
0 1 4 15 0 1 4 15
Hours of incubation
MG 132(-)
MG 132(+)

FIGURE 6

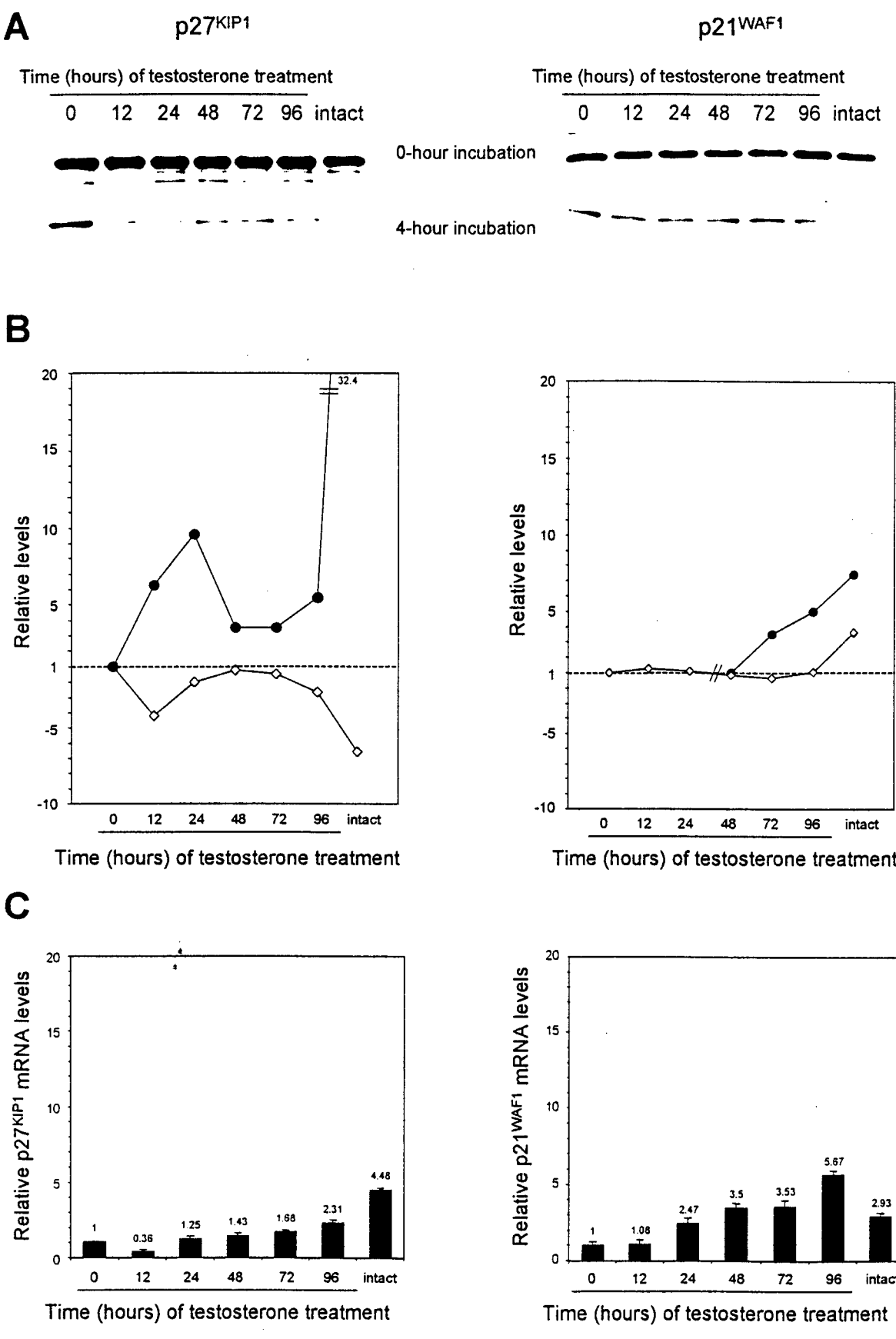
A
p27KIP1
p21WAF1
Time (hours) of testosterone treatment
0 12 24 48 72 96 intact
0-hour incubation
4-hour incubation
B
Relative levels
32.4
Time (hours) of testosterone treatment
C
Relative p27KIP1 mRNA levels
1
0.36
1.25
1.43
1.68
2.31
4.48
Relative p21WAF1 mRNA levels
1
1.08
2.47
3.5
3.53
5.67
2.93

FIGURE 7

DEPARTMENT OF THE ARMY
US ARMY MEDICAL RESEARCH AND MATERIEL COMMAND
504 SCOTT STREET
FORT DETRICK, MARYLAND 21702-5012

REPLY TO
ATTENTION OF:

MCMR-RMI-S (70-1y) 8 Jan 2003

MEMORANDUM FOR Administrator, Defense Technical Information Center (DTIC-OCA), 8725 John J. Kingman Road, Fort Belvoir, VA 22060-6218

SUBJECT: Request Change in Distribution Statement

1. The U.S. Army Medical Research and Materiel Command has reexamined the need for the limitation assigned to the enclosed. Request the limited distribution statement for the enclosed be changed to "Approved for public release; distribution unlimited." These reports should be released to the National Technical Information Service.

2. Point of contact for this request is Ms. Judy Pawlus at DSN 343-7322 or by e-mail at judy.pawlus@det.amedd.army.mil.

FOR THE COMMANDER:

PHYLLIS M. RINEHART
Deputy Chief of Staff for
Information Management

Encl

ADB265840

ADB266633

ADB282069

ADB279138	ADB251763	ADB265386
ADB264578	ADB281601	ADB282057
ADB281679	ADB258874	ADB258251
ADB281645	ADB281773	ADB264541
ADB261128	ADB281660	ADB241630
ADB261339	ADB259064	ADB281924
ADB273096	ADB266141	ADB281663
ADB281681	ADB281664	ADB281659
ADB259637	ADB258830	
ADB256645	ADB266029	
ADB262441	ADB281668	
ADB281674	ADB259834	
ADB281771	ADB266075	
ADB281612	ADB281661	